



Westaway, R. (2018) Deep geothermal single well heat production: critical appraisal under UK conditions. *Quarterly Journal of Engineering Geology and Hydrogeology*, 51(4), pp. 424-449. (doi:10.1144/qjegh2017-029)

There may be differences between this version and the published version. You are advised to consult the publisher's version if you wish to cite from it.

<http://eprints.gla.ac.uk/164303/>

Deposited on: 21 June 2018

Enlighten – Research publications by members of the University of Glasgow
<http://eprints.gla.ac.uk>

1 **Deep geothermal single well heat production: critical appraisal under UK conditions**

2
3 **Rob Westaway**

4 School of Engineering, University of Glasgow,
5 James Watt (South) Building, Glasgow G12 8QQ, U.K.

6
7 **e-mail: robert.westaway@glasgow.ac.uk**

8 **Abstract**

9 The idea of Deep Geothermal Single Well (DGSW) heat production has existed for many years, but
10 with no consensus regarding its potential applicability: proponents have made claims regarding
11 thermal outputs that appear exaggerated, whereas detractors have stated that the concept can never
12 be economic unless the capital cost of drilling has already been discounted. However, because this
13 technology offers the potential of delivering geothermal heat projects ‘off the shelf’ with a minimum
14 of site-dependent research, the possibility exists of achieving cost-effective solutions. The present
15 study sets out to investigate this topic subject to environmental and subsidy regimes applicable in the
16 UK; the results might also be useful for other jurisdictions. Under these conditions, the variant of the
17 technology with greatest potential for cost effectiveness is the hcDGSW, or conductive DGSW with
18 heat production via heat pump. Analytic modelling enables the physics of the heat-exchange
19 processes within a hcDGSW to be approximated. It is thus established that this option can indeed be
20 cost-effective under the current UK subsidy regime for deep geothermal heat, provided boreholes are
21 deep enough and in localities where the geothermal gradient is high enough. The environmentally
22 optimum operational mode (optimizing savings in CO₂e emissions) involves heat production at a lower
23 rate than the economically optimum mode (maximizing profit). If such projects are subsidized from
24 public funds, then a particular operational mode might be specified, maybe as a compromise between
25 these optima. After the 20 year duration of the subsidy, the technology might well no longer be
26 economic, but the infrastructure might be easily repurposed for seasonal heat storage, thus offering
27 the potential of making a significant long-term contribution to sustainable future heat supply. These
28 preliminary results indicate that more detailed appraisal of this technology variant is warranted.

29 30 **Introduction**

31 Most deep geothermal heat production projects are based around the concept of well doublets, in
32 which production of thermal water from one well is balanced by injection of the water (after heat is
33 supplied from it to the heat load) in a second well. The injection of water serves two purposes: it
34 avoids the drawdown in hydrostatic pressure that would result in the geothermal reservoir rocks if
35 only a production well were in operation; it also avoids the need for treatment of the produced water
36 before surface disposal, which in many circumstances would otherwise be necessary. Typically one or
37 both of the injection and production wells are deviated so they reach the geothermal reservoir some
38 distance (up to ~2 km; e.g., Smit, 2012) apart. Over time a project of this type gradually extracts heat
39 from the reservoir rocks surrounding the production well; heat production usually takes place far
40 faster than the associated ‘thermal recharge’ by upward heat flow from the Earth’s interior. The cold
41 thermal front emanating from the injection well will therefore eventually reach the production well,
42 limiting the lifetime of the project (e.g., McDermott et al., 2006; van Wees et al., 2010; Satman, 2011;
43 Smit, 2012). Used in this manner, this technology is thus not indefinitely ‘sustainable’ but is
44 nonetheless regarded by most authorities as providing ‘renewable’ energy and therefore in principle
45 eligible for subsidies (e.g., the UK government’s Renewable Heat Incentive or RHI) designed to
46 stimulate the development of ‘low carbon’ heat sources.

47
48 Such development requires the identification of reservoir rocks at appropriate temperatures and with
49 suitable physical properties (porosity and permeability, or hydraulic conductivity, associated with
50 fractures or pore spaces) to enable heat production at useful rates; it thus involves exploitation of
51 complex systems that may well not be understood until the development is under way (e.g., Tenzer

1 et al., 2010), and thus requires considerable technical skill. If suitable properties do not exist naturally
2 they can in principle be created by techniques such as hydraulic fracturing, acid injection (to dissolve
3 carbonate cement and increase pore space within rocks), or thermal fracturing (injection of cold water
4 so thermal contraction causes fracturing of the rocks). However, hydraulic fracturing can cause
5 induced seismicity and acid injection might cause environmental pollution; projects using these
6 techniques might thus attract opposition. Commercial deep geothermal projects have nonetheless
7 come on stream in western Europe. Examples include Soultz-sous-Forêts and Rittershoffen in eastern
8 France (e.g., Vidal et al., 2016; Baujard et al., 2017), which have used the aforementioned well
9 stimulation techniques, and many deep geothermal heat projects in the Netherlands (e.g., Bleiswijk;
10 Ramaekers et al., 2006; Simmelink and Geel, 2008; Donselaar et al., 2015). However, each of these
11 examples has depended on prior knowledge of rock properties from petroleum exploration. Since heat
12 is inherently a less valuable commodity than oil or natural gas, it is more problematic whether a project
13 of this type could be implemented on a commercial basis in a region that has not previously been
14 documented in detail for this reason, such as most of the onshore UK, since the cost of the necessary
15 site-dependent research might never be recoverable from the value of the heat that could be
16 produced (cf. King et al., 2015). For both these reasons, the UK will benefit from any alternative
17 approach to geothermal development that is uncontroversial and straightforward to implement ‘off
18 the shelf’, without detailed site-dependent investigation.

19

20 The term Deep Geothermal Single Well (DGSW) denotes any geothermal project design that utilizes a
21 single borehole (rather than a doublet), and which extends into the ‘deep geothermal’ regime, which
22 under current UK regulations means depth >500 m (e.g., AECOM, 2013); many possible variants exist,
23 including both open- and closed-loop designs (Table 1; Figs. 1, 2, 3). Some of these variants extract
24 heat by conduction from the rocks around any borehole (Fig. 3; see, also, below), making them
25 potentially straightforward to implement (since they do not depend on knowledge of hydraulic
26 transport properties); furthermore, no ‘well stimulation’, such as hydraulic fracturing, is necessary.
27 This technology is thus potentially suitable for providing ‘off the shelf’ geothermal heat sources in the
28 UK, provided it can achieve an economic return. In the UK, heat output from a DGSW is eligible, in
29 principle, for RHI subsidy; this is currently (February 2017) £0.0514 kWh⁻¹. Recent works on this topic
30 include those by Law (2014), Law et al. (2015), GEL et al. (2016), and Collins and Law (2017). As will
31 become clear below, some aspects of these publications are open to question, including apparent
32 overestimation of outputs of useable heat and underestimation of system operating costs and impacts
33 of uncertainty in knowledge of rock properties at depth and regulatory issues. The present study seeks
34 to focus discussion on the variant of this technology (the hcDGSW; Table 1 and Fig. 2(b)) that is shown
35 to offer the greatest potential under present UK economic and regulatory conditions; the analysis
36 might also be useful in other jurisdictions. This investigation concentrates on underlying principles;
37 practical details, such as designs of components (e.g., pumps and heat exchangers) and wall
38 thicknesses of pipework (to handle the imposed fluid pressures and maintain the necessary thermal
39 insulation) are beyond the scope of the present study (see, e.g., Rafferty, 2001; Law et al., 2015;
40 Alimonti et al., 2016).

41

42 Many workers have published analyses of deep DGSW case studies, for production of either
43 geothermal electricity or geothermal heat (e.g., Nalla et al., 2004; Wang, 2009; Wang et al., 2010; Bu
44 et al., 2012; Cheng et al., 2013; Law et al., 2015, 2016; Alimonti and Soldo, 2016; Alimonti et al., 2016;
45 Cho et al., 2016; Noorollahi et al., 2016; Riahi et al., 2017). However, some of these analyses use
46 numerical modelling techniques that are either not explained or not validated against analytic
47 calculations, others incorporate non-physical assumptions such as constant-temperature boundary
48 conditions at depth or the assumption that these systems can operate under steady state.
49 Furthermore, some of these studies analyse the physics of heat exchange around and within boreholes

1 without considering how this heat transfer interacts with any heat load. However, it is clear from the
2 substantial literature on shallow borehole systems connected to heat pumps (e.g., Bloomquist, 1999;
3 Rees et al., 2004; Orio et al., 2005; O'Neill et al., 2006; Kavanaugh et al., 2012; Liu et al., 2016) that
4 borehole heat exchanger designs and heat loads should be matched, making it essential to consider
5 both in combination, rather than either in isolation, to achieve optimal solutions; this is shown in the
6 present study to also be so for deep borehole systems. In the absence of any established method, this
7 study will present an analytic approach for modelling both subsurface installations and heat loads for
8 deep DGSW installations, those aspects of the underlying physics that appear most important to the
9 author being included. Such an analytic approach incorporates exact solutions for particular aspects
10 of this coupled problem, which approximate the conditions that can be anticipated during the
11 operation of real DGSW installations. This approach might be useful for validating future numerical
12 solutions, but the immediate aim is to permit first-order assessments of recent DGSW investigations
13 in the UK (e.g., Law et al., 2015, 2016; Collins and Law, 2017), for which high heat outputs have been
14 reported. The existing literature on shallow systems (e.g., Rees et al., 2004; Banks, 2012) indicates that
15 the useable heat output increases with borehole depth, so higher values are expected for increasing
16 borehole depth, but the manner in which heat output scales with borehole depth has not hitherto
17 been established. Law et al. (2015, 2016) and Collins and Law (2017) have reported results of
18 numerical analyses that quantify the rates of heat production that they consider feasible for particular
19 borehole depths and bottom hole temperatures, but the software used has not been published, no
20 validation against analytical calculations has been reported, nor any indication of how heat production
21 depends on site conditions in general, or how much of the heat produced can provide output of
22 useable heat, bearing in mind that most designs involve reinjection of water and the heat it contains.

23
24 The Southampton geothermal project in southern England, dating from the early 1980s, was the first
25 to produce hot water from a deep borehole, discharging the cooled water into the environment,
26 rather than reinjecting it (e.g., Barker, 1986). As many authors (e.g., Downing et al., 1984; Downing,
27 1986; Barker et al., 2010) have discussed, the Southampton-1 borehole reaches permeable Triassic
28 sandstone at 76 °C at 1827 m depth. Well-testing established that this aquifer would be unlikely to
29 sustain the high flow rates originally envisaged, which would have provided several megawatts of heat
30 output using a conventional well doublet. It was therefore decided to develop this single borehole as
31 a heat source (wellhead temperature 74 °C) for district heating, discharging the produced water into
32 the sea. In its original form (here designated as wdGSW; Fig. 1(a)) this project had a useable heat
33 output of ~1.15 MW (Barker et al., 2010). It was modified in 1991 with the addition of a heat pump
34 (to the hwDGSW configuration in Fig. 1(b)); by reducing the temperature at which the produced water
35 is rejected to the environment, this increased the output of useable heat to ~2.2 MW (Barker et al.,
36 2010), the flow rate required for this being ~7.5 l s⁻¹.

37
38 Although the Southampton-1 produced water is not treated, in general in the UK treatment of
39 produced water from deep geothermal projects will be necessary before discharge into the
40 environment (e.g., Atkins, 2013). For example, the radionuclide ²²⁶Ra is one of its more potentially
41 hazardous constituents, since radium is chemically similar to calcium and so can participate in many
42 chemical reactions in the environment. According to Edmunds (1986), the Southampton-1 well
43 produces 39 picocuries of ²²⁶Ra per kg of water, equivalent to ~1.4 Bq kg⁻¹ or ~1.4 Bq l⁻¹. At ~7.5 l s⁻¹,
44 this well thus discharges ~340 MBq of alpha radiation from ²²⁶Ra per year. The relevant regulations
45 (DEFRA, 2011, p. 81) permit discharges with ²²⁶Ra activity of up to 100 Bq l⁻¹ for this purpose, although
46 in water produced as a by-product of hydrocarbon production any concentration above 1 Bq l⁻¹ would
47 require treatment. Edmunds (1986) also reported the concentration of iron in this water as 4.1 mg l⁻¹.
48 For each chemical contaminant, such as this, the regulatory requirement is for concentration in the
49 water body receiving the discharge to not exceed a specified limit, which for iron is 1 mg l⁻¹ (e.g.,
50 DEFRA, 2014). Since the Southampton discharge is into the sea, the dissolved iron is evidently diluted
51 sufficiently for compliance. However, the present regulatory presumption is that no additional

1 discharge should adversely affect any water body, which effectively means that concentrations in the
2 discharge should not exceed the regulatory limit for the water body. Thus, as Atkins (2013) noted,
3 'discharge to surface without treatment is unlikely to be a viable option' for future DGSW systems in
4 the UK. The UK has a widespread legacy of mining, which has caused many discharges of groundwater
5 that do not comply with present environmental standards and so now require treatment (e.g.,
6 Younger et al., 2005). As Johnston et al. (2008) have explained, this situation arose as a consequence
7 of an ambiguous legal framework concerning responsibility for historical discharges, which was
8 rectified for future discharges by a change to the law in 1999. This situation thus provides no
9 precedent for tolerating untreated discharges from future DGSW systems (see, also, Atkins, 2013, and
10 Abesser et al., 2014); indeed, knowledge of mine water treatment costs can inform discussion of
11 potential treatment costs for water discharged from these systems (see below).

12
13 Heat might also be extracted by conduction from the rocks surrounding a borehole heat exchanger,
14 containing a closed loop of heat transfer fluid, a variant of the technology (depicted schematically in
15 Fig. 2(a)) designated here as a conductive DGSW or cDGSW. As far as can be established, this idea was
16 first proposed by Lockett (1986). This author reported that circulation of 'special fluids' within a
17 borehole in rocks at a temperature of 150 °C might produce sufficient heat for electricity generation
18 at 2.5 MW, a claim that was unsupported by calculations and seems exaggerated (cf. Alimonti et al.,
19 2016). A similar concept was independently studied by Rybach et al. (1992); these authors estimated
20 the potential heat output as so low that this technology would in their view never be economic if
21 drilling costs were included, but might be viable when applied to existing boreholes, for example 'dry'
22 hydrocarbon wells or unsuccessful conventional geothermal boreholes. As Westaway (2016) noted,
23 an attempt was made in 2011 to patent the cDGSW concept; it lapsed, presumably because the
24 applicant became aware that the idea was not original. Law et al. (2015) noted that the cDGSW
25 concept offers the potential for 'off the shelf' geothermal heat sources that require minimal site-
26 specific investigation, potentially speeding up the adoption of geothermal energy in the UK. Most
27 recently, the Glasgow-based energy company Geothermal Power Ltd.
28 (<http://geothermalpowerltd.com/>) has advocated cDGSW use for electricity generation and that they,
29 too, are in the process of patenting the technology. In principle, a cDGSW installation might be
30 combined with a heat pump, to increase the output of useable heat from the resulting hcDGSW (Fig.
31 2(b)) although (again, as far as can be established) there has been no published analysis of the
32 potential output or economic viability of this DGSW variant.

33
34 A further recent development (e.g., Law et al., 2015; GEL et al., 2016) has been the variant (which
35 might be termed the 'dual mode' DGSW, or dDGSW; Fig. 3(a)), with the borehole heat exchanger left
36 open around its base so the heat production that is feasible from a cDGSW can be supplemented by
37 'bleed flow' of thermal ground water. GEL et al. (2016) have since proposed a further hdDGSW variant
38 with a heat pump (Fig. 3(b)). They deduced that this might be economically viable with RHI subsidy
39 payments, although their analysis omitted water treatment costs. However, the need for permeable
40 bedrock for these variants to function, plus the site-specific nature of the options for treating the
41 produced water, negate the original objective of providing 'off the shelf' geothermal heat. Collins and
42 Law (2017) have discussed two such projects, for a hdDGSW installation in the Aberdeen Granite
43 beneath the Aberdeen Exhibition and Conference Centre (AECC) in the Scottish city of Aberdeen, and
44 for a scheme to heat part of an outdoor swimming pool in Penzance, Cornwall, involving drilling into
45 the Land's End Granite, also mentioning a project in East Ayrshire, Scotland. Planning documentation
46 (Cornwall, 2017; East Ayrshire, 2017; Geon, 2017) indicates that the Penzance scheme has a dDGSW
47 design, whereas the latter project, now known as HALO and located in the town of Kilmarnock (where
48 drilling into Palaeozoic sedimentary rocks is proposed), is intended to function as a hcDGSW (see
49 below).

1 This proliferation of alternatives (Figs. 1, 2, 3) has created a somewhat confused situation, especially
 2 as workers have not always been clear which variant is being described in a given document and some
 3 aspects, such as treatment of produced water, have not received sufficient attention. Furthermore,
 4 the contrasting claims regarding thermal output and economic viability or otherwise require
 5 resolution, especially as not all variants (including the hcDGSW) have been fully analysed. The present
 6 study sets out to address these issues. It will, first, present a quantitative evaluation, using analytical
 7 calculations, of the potential output of a hcDGSW (Fig. 2(b)) relative to a cDGSW (Fig. 2(a)). Second,
 8 two key issues affecting the viability of the alternative dDGSW variant, the low hydraulic conductivity
 9 of many lithologies and the potential cost of produced water treatment, will be discussed. Third, the
 10 analytical model for a hcDGSW, the technology variant shown to have the most potential, will be used
 11 to develop an economic model for assessing effectiveness in terms of both cost and greenhouse gas
 12 emissions. Finally, the cDGSW/hcDGSW conceptual model by Law et al. (2015) and some individual
 13 DGSW projects will be discussed in the light of the preceding analyses. Given the approximations made
 14 in the aforementioned analytical calculations, the potential merits of the hcDGSW variant, thus
 15 identified, require confirmation by more detailed numerical modelling, beyond the scope of the
 16 present study.

18 cDGSW Theory

19 A cDGSW can be envisaged as a closed loop formed by inserting a length of pipe into a cased borehole,
 20 as in Fig. 2(a). Water (or, possibly, an alternative heat transfer fluid; e.g., Alimonti and Soldo, 2016) is
 21 produced from the borehole at temperature T_o and supplied to a surface heat exchanger that extracts
 22 heat to the heat load at its operational temperature T_E . The water (or other circulating heat-transfer
 23 fluid) is thus itself cooled to T_E within the heat exchanger before reinjection at temperature T_D . As Law
 24 et al. (2015), Alimonti and Soldo (2016), and other workers have discussed, a suitable configuration
 25 has the upward flow in a central pipe within the well, with the downward flow in the surrounding
 26 annulus (Fig. 2(a)). During its downward flow the circulating fluid absorbs heat from the surrounding
 27 rocks; during its upward flow, which might be much faster if the pipe is much narrower than the
 28 annulus, it is assumed (for calculation purposes) that the fluid maintains temperature T_o . In principle,
 29 a cDGSW (and, indeed, any other variant of DGSW) might operate intermittently, possibly delivering
 30 heat on diurnal or seasonal cycles. However, since the thermal processes involved are governed by
 31 linear equations, after many such cycles the thermal state around a DGSW will be indistinguishable
 32 from that which would exist had it been operated to produce heat at a constant rate equal to the
 33 time-averaged rate for the actual pattern. The development of theory will therefore assume heat
 34 production at a constant rate.

35
 36 Law et al. (2014) showed by field testing that in such a configuration the downward flow maintains
 37 roughly constant temperature T_D until it reaches a depth z_L where the initial temperature of the
 38 surrounding rock T_L equals T_D . Thus, between the Earth's surface and depth z_L the return flow heats
 39 this surrounding rock, and therefore only between z_L and the well bottom at depth z_M is heat extracted
 40 from the surrounding rock. This turns out to be a significant limitation of the cDGSW concept (see
 41 below). To facilitate the analysis, the ratio z_L / z_M is designated as f ; the proportion of the borehole
 42 that acts as a heat source is thus $1-f$.

43
 44 The general equation governing heat flow in cylindrical polar co-ordinates is

$$45 \frac{\partial T}{\partial t} = \kappa \left(\frac{\partial^2 T}{\partial r^2} + \frac{1}{r} \frac{\partial T}{\partial r} + \frac{1}{r^2} \frac{\partial^2 T}{\partial \theta^2} + \frac{\partial^2 T}{\partial z^2} \right), \quad (1)$$

46
 47 where T is temperature, t is time, κ and k are the thermal diffusivity and conductivity of the rock
 48 around a borehole, and r , θ and z are radial distance (from the axis of a borehole), azimuth, and depth.
 49 The solutions assume no azimuthal dependence, also that the abrupt radial temperature gradients
 50

1 $(\partial T/\partial r)$ that can be expected beyond the borehole radius a are much greater than the vertical
 2 geothermal gradient, so the latter is neglected. Equation (1) can thus be simplified to

$$3 \frac{\partial T}{\partial t} = \kappa \left(\frac{\partial^2 T}{\partial r^2} + \frac{1}{r} \frac{\partial T}{\partial r} \right) \quad (2)$$

6 Starting at time $t=0$, when radial temperature gradients first develop, heat is assumed to flow inward
 7 across the boundary at $r=a$ at a steady rate Λ , per unit surface area of the borehole, or at rate ζ per
 8 unit depth, where $\zeta = 2 \pi a \Lambda$ ($2 \pi a$ being the circumference of the borehole). The resulting net heat
 9 production is the sum of all these contributions across the depth range from z_L to z_M . Equation (2) has
 10 been solved subject to these boundary conditions by many workers (e.g., Carslaw and Jaeger, 1959,
 11 pp. 338-341). The solution can be expressed in terms of combinations of a decaying exponential
 12 function of time and Bessel functions of radial distance, and has no simple general form. However,
 13 Carslaw and Jaeger (1959) found power series approximations that are valid, separately, in the limits
 14 of $t \ll r^2/\kappa$ and $t \gg r^2/\kappa$. The latter solution, valid at (relatively) long timescales after $t=0$, can be written
 15 as

$$16 \Delta T(r,t) = \frac{-\Lambda a}{2k} \left(\ln \left(\frac{4\kappa t}{Cr^2} \right) + \frac{a^2}{2\kappa t} \ln \left(\frac{4\kappa t}{Cr^2} \right) + \frac{1}{4\kappa t} (a^2 + r^2 - 2a^2 \ln \left(\frac{a}{r} \right)) \right), \quad (3)$$

19 where ΔT is the temperature change from the initial conditions and $C \equiv \exp(\gamma)$, γ being Euler's constant
 20 ($\sim 0.57722\dots$). For $t \gg r^2/\kappa$, this solution can be approximated further and rewritten in terms of ζ as

$$21 \Delta T = \frac{-\zeta}{4\pi k} \ln \left(\frac{4\kappa t}{Cr^2} \right). \quad (4)$$

24 Furthermore, if ζ is assumed to be zero at depth z_L and to increase linearly to a maximum value ζ_M at
 25 depth z_M , then

$$26 \zeta_M = \frac{2Q}{z_M(1-f)}. \quad (5)$$

29 ΔT will thus be proportional to depth beneath z_L . The temperature of the water produced from the
 30 borehole, T_o , will therefore equal the initial temperature T_M at depth z_M , minus ΔT calculated using
 31 equation (4) for $r=a$ and $z=z_M$ so $\zeta=\zeta_M$. It follows that the rock at $r=a$ at all depths $z_L \leq z \leq z_M$ will cool to
 32 the same limiting temperature in the limit of $t \rightarrow \infty$. This clearly approximates reality, as it implies a
 33 step change in T at depth z_M ; the importance of this approximation is addressed below.

35 To summarize the underlying physics, the heat production from the borehole, at rate Q , occurs as a
 36 result of the warming of the circulating fluid as it flows downward, absorbing heat through the outer
 37 wall of the borehole heat exchanger. This fluid then flows upward along the inner pipe of the heat
 38 exchanger, maintaining the same flow rate q_c as no 'bleed flow' into the borehole is assumed. For
 39 plausible operational modes of cDGSW or hcDGSW installations, the upward flow along this inner pipe
 40 (of internal diameter D) will be turbulent (see below), so will approximate a uniform velocity profile
 41 V ; q_c can thus be approximated as $\pi V D^2 / 4$. If the circulating fluid is injected at temperature T_D and
 42 produced at temperature T_o , the rate of heat production will balance the rate of heat gain by the
 43 circulating fluid; thus

$$45 Q = \rho c (T_o - T_D) q_c, \quad (6)$$

47 where ρ and c are the density and specific heat capacity of this fluid. The value of q_c that is required
 48 for a given cDGSW or hcDGSW installation to operate at a given rate of heat production Q is calculated
 49 by rearranging equation (6), thus

$$q_c = \frac{Q}{\rho c (T_o - T_D)} \quad (7)$$

Since T_o will decrease over time (as in Fig. 4), operational modes at constant Q require progressive increases in q_c over time, given that ρ , c and T_D are assumed to remain constant.

The workflow for present modelling approach involves specifying z_M , a , and D for the borehole, T_s , T_M , k , and κ for the surrounding rock volume, ρ and c for the circulating fluid, and T_D from the characteristics of the surface heat exchanger installation. For each candidate rate of heat production Q , T_o is calculated for a succession of times t using equations (4) and (5), with the corresponding value of q_c determined using equation (7). This differs, for example, from the numerical modelling approach used by Alimonti and Soldo (2016), for which constant q_c is specified and Q , at rates that decrease progressively over time, calculated from it. The present solution nonetheless incorporates the essential physics governing the energy balance for a cDGSW, whereby the heat produced in the flow through a borehole heat exchanger is equal to the heat lost by conduction from the surrounding rock volume.

Nonetheless, although this analytic solution maintains conservation of energy overall, it does not attempt to balance energy for any part of the model. For example, no attempt is made to explicitly model the progressive warming of the circulating fluid as it flows downward along the outer pipe (Fig. 2) or the cooling of the fluid flowing upward along the inner pipe as heat flows radially outward from it into its lower-temperature surroundings (cf. Alimonti et al., 2016). Furthermore, it is evident that (in addition to the pre-existing geothermal gradient) vertical temperature gradients will develop within the rock volume surrounding the borehole, meaning that the approximation used to justify equation (2) will not be valid. Each of these aspects will cause complexity that is not incorporated into the analytic model.

Differentiating equation (4) with respect to r gives

$$\frac{\partial \Delta T}{\partial r} = \frac{\zeta}{2 \pi k r} \quad (8)$$

As time progresses, the volume of rock cooled thus gradually widens, but equation (8) means that the induced radial geothermal gradient increases inward, so the temperature gradient around the borehole will draw heat in from farther out (Fig. 5). Thus, although the borehole becomes surrounded by an ever-widening volume of cooled rock, this radial geothermal gradient will always direct heat inwards towards it. Nonetheless, the operational lifespan of a cDGSW, the time over which it can produce heat before the temperature at $r=a$ cools below any value that is useful, turns out to be very sensitive to choices of parameter values (see below). It is also noteworthy that although Q is the rate of heat production from the borehole, it will only equal the rate of heat output to the load if $f=0$, i.e., if the reinjection temperature T_D equals the ambient surface temperature T_s . Otherwise, only a proportion f , equal to $(T_o - T_L) / (T_o - T_s)$ of Q will be output to the load and the remainder will be reinjected, contributing (as already noted) to heating the rock volume at $z < z_L$. Thus, as the rock volume at $z > z_L$ gradually cools, T_o will eventually (at time t_L) decrease to T_L , at which point the DGSW will cease to deliver any useable heat output, effectively ending its useful life. At this point $\Delta T(z_M) = T_L - T_M$; substituting this condition into equation (4) and using equation (5), followed by other algebraic steps including recognizing that $T_M - T_L = (1-f) (T_M - T_s)$ and that $T_M - T_s = u z_M$, where u is the geothermal gradient, gives

$$t_L = \frac{C a^2}{4 \kappa} \exp \left(\frac{2 \pi k (1-f)^2 z_M^2 u}{Q} \right) \quad (9)$$

1 The exponential term in equation (9) means that t_L , thus calculated, is indeed very sensitive to choices
 2 of parameter values, as is illustrated in Fig. 6.

3
 4 The algebraic threshold of validity of the above 'long-timescale' solutions, at $t=r^2/\kappa$, corresponds to
 5 quite short timescales when r is small; for example, at $r=a=0.1$ m and with $\kappa=1$ mm² s⁻¹ it is 10000 s or
 6 circa 2 hours 47 minutes. This solution is therefore applicable near the borehole on all timescales
 7 relevant to cDGSW operation. On the other hand, the use of equation (4) to determine the radius r_c
 8 of this cooling effect, is more problematic. Equation (4) implies that $\Delta T=0$ when $r=r_c$, thus

$$9 \quad r_c = 2 \sqrt{\frac{\kappa t}{C}}. \quad (10)$$

10
 11 Plots of the function described by equation (4) indeed show that as r approaches r_c the value of $\partial\Delta T/\partial r$
 12 is significant (Fig. 5), so $\partial\Delta T/\partial r$ has a discontinuity at $r=r_c$ which has no physical basis. The higher-order
 13 approximation in equation (3) also breaks down in the vicinity of $r=r_c$; this function indeed never
 14 actually satisfies $\Delta T=0$, it instead has a turning point beyond which ΔT starts to diverge away from
 15 zero. After several algebraic steps this can be shown to occur at $r=r_c$ where

$$16 \quad r_c^2 = 4 \kappa t + a^2. \quad (11)$$

17
 18 For operation of any significant duration, $r_c^2 \gg a^2$, thus

$$19 \quad r_c \approx 2 \sqrt{\kappa t}. \quad (12)$$

20
 21 The estimate of r_c from equation (12) is thus \sqrt{C} times, or ~ 1.33 times, that from equation (10).

22
 23 It is also relevant that the solution for an infinitesimally thin 'line source', emitting or absorbing heat
 24 at a rate ζ per unit length, is

$$25 \quad \Delta T = \frac{\zeta}{4 \pi k} E_1(r^2 / (4 \kappa t)) \quad (13)$$

26 (e.g., Carslaw and Jaeger, 1959, p. 261), where $E_1(\chi)$ is the exponential integral function. As r becomes
 27 larger this will be a close approximation to the solution for a heat source (or sink) of finite radius.
 28 However, since $E_1(0) \rightarrow \infty$ this equation is not physically meaningful at small values of r . Furthermore,
 29 although $E_1(\chi)$ decreases to very small values as χ increases, it never reaches precisely zero. $E_1(\chi)$ can
 30 be accurately approximated (for $\chi \geq 1$) as $\exp(-\chi) \times \ln(1 + 1/\chi)$ (e.g., Abramowitz and Stegun, 1964, p.
 31 229); for example, it is thus ~ 0.25 for $\chi=1$, ~ 0.05 for $\chi=2$, ~ 0.01 for $\chi=3$, and ~ 0.004 for $\chi=4$. Given that
 32 the term $\zeta / (4 \pi k)$ is of the order of 1 °C (see below) and a representative decrease in the temperature
 33 adjoining a DGSW can be a few tens of degrees Celsius (say, ~ 50 °C; see below), $\chi=1$ roughly
 34 corresponds to a temperature perturbation $\sim 0.5\%$ as large as that adjoining the borehole and can thus
 35 provide an alternative estimate of the effective value of r_c . One thus obtains $r_c^2 / (4 \kappa t) \approx 1$, indicating
 36 the same value for r_c as is given by equation (12).
 37
 38
 39
 40
 41
 42

43 A further complicating factor is that in addition to the radial cooling at $z \leq z_M$, cDGSW operation will
 44 cool the rock volume at depth $z > z_M$, which will add to the heat produced. An approximate correction
 45 will now be derived for this effect, in which it is assumed that this downward cooling effect extends
 46 over a depth range r_c below the well bottom at depth z_M , with its radius r_E and the associated
 47 temperature perturbation tapering linearly from r_c and ΔT at depth z_M to zero at depth z_M+r_c . Vertical
 48 position w within this cooled zone is measured upwards from zero at $z=z_M+r_c$. The cooling at each
 49 value of w can be approximated very crudely as extending over a radial distance out to $r=w$ with the

1 temperature perturbation proportional to $(w - r)^2/w^2$. The heat dE lost by cooling a cylindrical shell at
 2 vertical position y and radius r , of infinitesimal thickness dy and dr , can thus be estimated as

$$3 \quad dE = \Delta T(r=a, z=r_c) \rho c \frac{w}{r_c} \frac{(w-r)^2}{w^2} 2\pi r dr dw \quad (14)$$

6 where ρ and c are the density and specific heat capacity of the surrounding rock. Substituting for ΔT
 7 from equation (4) and using equations (5) and (10), together with $\kappa \rho c \equiv k$, one obtains

$$8 \quad E(t) = \frac{2 Q \ln(r_c/a)}{z_M \kappa (1-f) r_c} \int_{w=0}^{r_c} w \int_{r=0}^{w-r} \frac{(w-r)^2}{w^2} r dr dw \quad (15)$$

11 as an estimate for the total heat lost by cooling of this borehole end zone from time zero up to time
 12 t . After multiple algebraic steps, one obtains

$$13 \quad E(t) = \frac{Q}{12 z_M \kappa (1-f)} \ln\left(\frac{4 \kappa t}{C a^2}\right) \left(\frac{4 \kappa t}{C}\right)^{1.5} \quad (16)$$

16 or

$$17 \quad E(r_c) = \frac{Q}{6 z_M \kappa (1-f)} \ln\left(\frac{r_c}{a}\right) r_c^3 \quad (17)$$

21 The effect of this contribution can be illustrated using a representative example with $Q=100$ kW,
 22 $z_M=2500$ m, $\kappa=1$ mm² s⁻¹, $a=0.1$ m, and $t=20$ years, a realistic representative lifespan for a cDGSW (see
 23 below). Over this period of time the uncorrected heat production will thus be 100 kW \times 20 years or
 24 ~ 63.2 TJ. With these values, r_c will be ~ 37.7 m after 20 years, and the additional heat production, from
 25 the borehole 'end correction', will be ~ 2.1 TJ. Including this correction would thus only change the
 26 estimated overall heat production on this timescale by $\sim 3\%$. Over time scales such as this, the
 27 correction is so small that the various approximations made in its derivation are not of major
 28 importance. The essential reason for this is that on these time scales the roughly cone-shaped zone at
 29 the base of the borehole, whose heat loss is calculated as this correction, is very small compared with
 30 the cylindrical volume flanking the borehole, whose heat loss was calculated previously.

32 A further correction is necessary to incorporate the upward geothermal heat flow $k \times u$. After time t
 33 the rock volume cooled, of radius r_c , will present a horizontal cross-sectional area πr_c^2 to this heat
 34 flow. The borehole will thus 'capture' a heat flux of

$$35 \quad Q_G = \pi r_c^2 k u, \quad (18)$$

38 For $u=32$ °C km⁻¹ (the value adopted by Law et al., 2015, representative of geothermal gradients in
 39 radiothermal granites in different parts of Britain; e.g., Lee, 1986; Lee et al., 1987; Manning et al.,
 40 2007) and $k=3.5$ W m⁻¹ °C⁻¹ (likewise, a typical value for granitic rocks; e.g., Lee, 1986; Wheildon and
 41 Rollin, 1986; Lee et al., 1987; Manning et al., 2007) after 20 years, when r_c is again 37.7 m, the resulting
 42 additional heat flux will be ~ 500 W; this effect is thus even smaller in magnitude than the borehole
 43 'end correction'. However, if a cDGSW were designed with very low heat production and a very long
 44 lifespan, r_c would ultimately become so large that the geothermal heat flux 'captured' might balance
 45 the heat production, creating the possibility of a steady state situation. Equating Q_G in equation (18)
 46 to Q and using equation (10) for r_c , one obtains

$$47 \quad t_E = \frac{C Q}{4 \pi k \kappa u} \quad (19)$$

50 Taking reasonable estimates ($k \sim 3.5$ W m⁻¹ °C⁻¹, $\kappa \sim 1$ mm² s⁻¹, $u \sim 32$ °C km⁻¹, as before), one can
 51 estimate that t_E is ~ 40 years per kilowatt of heat production Q . This steady-state limiting behaviour is

1 thus only relevant for extremely low heat production, being (for example) ~ 1000 years for $Q=25$ kW,
2 by which time the cooled volume will have widened to $r_c \sim 270$ m. Such limiting behaviour is an
3 interesting scientific curiosity, but does not help with the assessment of how cDGSW technology might
4 be used to produce worthwhile heat outputs on timescales of practical interest.

5 6 *Discussion*

7 Figure 4 illustrates the predicted variation in output temperature for a cDGSW, for its first ten years
8 of operation at a range of constant heat production rates. Over this timescale, the radius of the
9 cylindrical rock volume cooled by the operation of the DGSW (Fig. 5) is so small that the
10 aforementioned corrections for heat flow and for cooling at greater depths have no significant effect.
11 Figure 4 thus illustrates a progressive decline in output temperature as the rock volume around the
12 cDGSW progressively cools, the decrease on a given timescale being proportional to the heat
13 production, as is to be expected from the linear governing equation (equation (2)). Figure 5 confirms
14 that the thermal state of the rock volume surrounding a cDGSW progressively evolves over time, with
15 no indication that it reaches a steady state on timescales of decades, although (as noted above) a
16 steady state might ultimately be attained after thousands of years. Nonetheless, both Fig. 4 and Fig. 5
17 demonstrate that after years of operation of a cDGSW the rates of cooling in and widening of the
18 surrounding affected rock volume will have become very low; Alimonti et al. (2016) described this
19 behaviour as an 'almost steady state condition'.

20
21 Figure 6 demonstrates that the performance of a cDGSW depends strongly on its mode of use; if fluid
22 is reinjected at a temperature above the value T_s at the Earth's surface (i.e., $f>0$), the duration over
23 which a given rate of heat production can be maintained is significantly reduced. This means that the
24 performance of any such installation cannot be analysed in isolation, but must be considered in
25 conjunction with the manner in which the heat output is used. The optimum situation is to reinject
26 fluid at T_s (i.e., $f=0$). However, since any real heat load will operate at a temperature T_E significantly
27 above T_s , reinjection at $f=0$ will require use of a heat pump (interfacing between the borehole
28 circulation loop and the heat load) to lower the temperature of the fluid circulating back into the
29 borehole below T_E , ideally to T_s . This is the essential reason why the hcDGSW configuration (Fig. 2(b))
30 is preferable to the simpler cDGSW variant (Fig. 2(a)). It has previously been noted (e.g., Collins and
31 Law, 2017) that DGSW heat outputs should be interfaced through heat pumps, but the essential
32 underlying physical reason has not previously been explained. The cost of the electricity required for
33 powering the heat pump therefore needs to be factored into any economic analysis (see below). The
34 electrical energy thus used will be converted to heat, contributing to the heat output supplied to the
35 load, also influencing the analysis.

36
37 Table 2 illustrates in more detail the performance issues that arise when the heat output from a
38 cDGSW supplies a heat load at a temperature T_E that significantly exceeds the surface temperature T_s
39 (i.e., $f>0$), for various values of z_M and T_M . Heat production from the cDGSW is thus assumed to occur
40 at rate Q , supplying a heat exchanger operating at a constant temperature $T_E=30$ °C, with no heat
41 pump. In all cases, the output temperature T_o from the cDGSW decreases over time at a rate that is
42 sensitive to Q . The proportion of the heat production that forms useable heat output, Q_U , is estimated
43 as $Q \times (T_o - T_E) / (T_o - T_s)$ and thus becomes ever smaller as T_o decreases, even though Q is assumed
44 constant. These results indicate that optimal cDGSW operation is quite sensitive; if Q is too high
45 relative to z_M and T_M the cDGSW will cool so quickly that Q_U is limited, whereas if Q is too low Q_U will
46 likewise be minimal. For a model cDGSW with $z_M=2500$ m and $T_M=90$ °C, with $T_E=30$ °C, the optimum
47 value of Q to maximise the useable heat output over 5 years turns out to be ~ 160 kW, decreasing to
48 ~ 140 kW if the timescale is set to 20 years. This model cDGSW might thus produce a steady output of
49 useable heat over 20 years of ~ 70 kW or thereabouts, by initially operating at $Q \sim 80$ kW then gradually
50 increasing Q to ~ 140 kW as the surrounding rock volume cools. Table 2 also shows the corresponding

1 values for $z_M=2000$ m, for which the maximum feasible steady output of useable heat over 20 years
2 would be only ~ 30 kW, and for $z_M=3000$ m, for which it would be ~ 130 kW.

3
4 For the three cDGSW configurations discussed above, the outputs of useable heat over 20 years can
5 be estimated, respectively, as ~ 22.8 , ~ 12.3 and ~ 5.3 GWh. At $\pounds 0.03$ per kWh, the value of the heat
6 produced would be $\sim \pounds 0.61$ M, $\sim \pounds 0.37$ M and $\sim \pounds 0.16$ M; if a RHI subsidy of $\pounds 0.0514$ per kWh were
7 included, these figures would rise to $\sim \pounds 1.86$ M, $\pounds 1.00$ M and $\sim \pounds 0.43$ M. The capital costs of these
8 projects might be estimated, respectively, as $\sim \pounds 2.9$ M, $\sim \pounds 2.3$ M and $\sim \pounds 1.8$ M (see below). It is thus
9 apparent (even before any estimation of operating costs) that such projects have no chance of being
10 cost-effective under current UK conditions. The calculations nonetheless exemplify that (over the
11 depth range considered) deeper cDGSW boreholes would be less uneconomic than shallower ones,
12 the increase in output of useable heat outweighing the corresponding increase in drilling costs, an
13 effect that is explored further later in this study.

14
15 A further point evident from Fig. 6 is that a small increase in the rate of heat production from a cDGSW
16 or hcDGSW can dramatically shorten its lifespan. This indicates that careful design, taking account of
17 the local geothermal gradient and other site-specific parameters, is essential. Assuming a given
18 borehole depth z_M , rate of heat production Q , and value of f , from equation (9) it is evident that the
19 project lifespan depends exponentially on the geothermal gradient u and on the thermal conductivity
20 k of the rock volume. A hcDGSW design that performs well at one site, with particular values of k and
21 u , might thus have a much shorter lifespan at another site with slightly lower k or u .

22
23 The figures for specific performance (i.e., heat output per unit length of borehole) warrant comparison
24 with those for 'ground source heat pump' systems utilising shallow-borehole (depth $< \sim 100$ m) heat
25 exchangers. The latter typically have specific performance of ~ 50 - 200 kWh m^{-1} yr^{-1} over annual
26 operating cycles (e.g., Hepbasli, 2005), or ~ 6 - 23 W m^{-1} . The hcDGSW designs being discussed have
27 higher specific performance, for instance 50 W m^{-1} for a 2000 m deep system with $Q=100$ kW. For
28 comparison, doublet systems might have heat outputs of many megawatts (say 8 MW from two
29 4000 m boreholes; e.g., van Wees et al., 2010), indicating a specific performance of 1000 W m^{-1} .
30 However, the overall energy balance is very different for shallow-borehole systems compared with
31 DGSW systems: the former can operate sustainably because of influxes of geothermal heat from
32 below and by surface heating from above, whereas (as noted above) for the latter the issue is not
33 sustainable operation but determination of the lifetime over which 'heat mining' is worthwhile. To
34 establish this, it is noted that a 50 m borehole with specific performance 10 W m^{-1} would have annual
35 heat output of ~ 16 GJ. From Fig. 5, a year of operation will cool the surrounding rock volume to a radial
36 distance of ~ 28 m, so will cool a cross-sectional area of ~ 2500 m^2 . A representative geothermal heat
37 flow is, say, ~ 90 mW m^{-2} or ~ 3 MJ m^{-2} yr^{-1} . Global warming and localized surface heating due to urban
38 development can cause downward heat flows from the surface that can exceed the upward
39 geothermal heat flux (e.g., Bayer et al., 2016; Westaway and Younger, 2016), amounting, say, to
40 ~ 4 MJ m^{-2} yr^{-1} . The combination of these flows might thus supply ~ 18 GJ yr^{-1} of heat into the ~ 2500 m^2
41 cross-sectional area, sufficient to balance the heat production. This essential difference, between
42 shallow-borehole systems that can operate sustainably and DGSW systems that 'mine heat', has not
43 been recognized before (cf. Collins and Law, 2017).

44 45 **Factors affecting dDGSW operation**

46 As already discussed, the alternative dDGSW variant (Fig. 3(a)) involves production of thermal ground
47 water to enhance the heat output that is feasible from conduction alone. Law et al. (2015) have indeed
48 suggested that heat production might be supplemented in this manner; for example, 'bleed flow' at
49 rate $q_B=2$ l s^{-1} at 50 °C above T_D would generate heat output of 2×10^{-3} m^3 $s^{-1} \times c \times \rho \times 50$ °C (where
50 $c=4186$ kg m^{-3} and $\rho=1000$ kg m^{-3} are the specific heat capacity and density of water; cf. equation (6))
51 or ~ 400 kW. Law et al. (2015) stated that $q_B=2$ l s^{-1} 'could be achieved from almost any geological

1 formation'. In the light of this, the hydraulic conductivity of relevant rock formations will now be
 2 discussed, along with the handling of the water produced from dDGSW projects, which might include
 3 treatment costs.

4
 5 *Effects of hydraulic conductivity*

6 Barker (1986) investigated the transient drawdown effect of a dDGSW, demonstrating that the
 7 required timescale is likely to be quite short. This topic can thus be analyzed, to place limits on the
 8 'bleed flow' that might be feasible, using the standard Thiem (1906) solution for the steady-state
 9 drawdown ΔH of the phreatic surface in a confined aquifer of transmissivity T_K in the vicinity of a
 10 production well:

$$11 \quad \Delta H = \frac{q_B}{2 \pi T_K} \ln\left(\frac{r_A}{r}\right). \quad (20)$$

14 Here, r_A denotes the 'radius of influence' of the aquifer, and r is again radial distance. Law et al. (2015)
 15 envisage placing an open (screened) section in the well casing of substantial vertical extent above the
 16 well bottom. The maximum drawdown in this layer, at $r=a$, can be designated as ΔH_0 . At distance from
 17 the borehole, the transmissivity of the layer in which this drawdown occurs will equal $K \times \Delta H_0$, where
 18 K is its hydraulic conductivity, from which it follows that the minimum value of K that can support the
 19 required flow rate under steady-state conditions is

$$20 \quad K = \frac{q_B}{2 \pi \Delta H_0^2} \ln\left(\frac{r_A}{a}\right). \quad (21)$$

23 Taking $\Delta H_0=100$ m, $r_A \sim 1$ km and $a=0.1$ m, for $q_B=2$ l s⁻¹ one obtains $K \sim 3 \times 10^{-7}$ m s⁻¹. Although some
 24 lithologies have K above this threshold, many in the UK and elsewhere do not (e.g., Allen et al., 1997;
 25 Lewis et al., 2006). Abesser et al. (2014) reached a similar conclusion, noting that water yields of ≥ 1 l s⁻¹
 26 are only feasible from boreholes in lithologies classified as 'moderate' or 'good' aquifers. Whether
 27 'bleed flow' can significantly supplement the limited heat output of a cDGSW is thus site-dependent
 28 and cannot be presumed in general. With $\Delta H_0=150$ m and $q_B=0.9$ l s⁻¹, equation (21) gives $\sim 6 \times 10^{-8}$ m s⁻¹
 29 as the hydraulic conductivity threshold for dDGSW operation to be feasible, indicating (as is evident
 30 from the form of equation (21)) that this threshold decreases as q_B is reduced or H_0 is increased. Coarse
 31 sediments might well thus have sufficient hydraulic conductivity for dDGSW operation to be feasible.
 32 For example, K has been reported as $\sim 10^{-5}$ m s⁻¹ in Triassic sandstone from southern England (e.g.,
 33 Smith, 1986); the operation of the aforementioned Southampton geothermal borehole as a wDGSW
 34 / hwDGSW indeed provides clear evidence of high K in such rocks.

36 Nonetheless, given that dDGSW projects have been proposed in granite, it is important to assess
 37 whether this lithology might have sufficient hydraulic conductivity for this technology to be feasible.
 38 It is indeed well known that intact granite at depth has very low K . For example, Brace et al. (1968)
 39 determined the permeability of Westerly Granite at ~ 50 MPa (roughly equivalent to ~ 2000 m depth)
 40 as ~ 63 nD ($\sim 6.3 \times 10^{-20}$ m²), equivalent (at ~ 70 °C, so water has a viscosity of ~ 0.4 mPa s) to
 41 $K \sim 4 \times 10^{-12}$ m s⁻¹. At 10 MPa (depth ~ 400 m), they measured its permeability as ~ 230 nD, indicating K
 42 $\sim 10^{-11}$ m s⁻¹. Martinez-Landa and Carrera (2005) reported that intact granite at the Grimsel Test Site in
 43 Switzerland, at ~ 450 m depth, has $K \sim 10^{-12}$ to $\sim 10^{-10}$ m s⁻¹, in good agreement. Such values are so far
 44 below any conceivable threshold required for a dDGSW or hdDGSW to function that this technology
 45 stands no chance of success in intact granite.

47 On the other hand, many workers (e.g., Martinez-Landa and Carrera, 2005; Hamm et al., 2007) have
 48 reported hydraulic conductivities orders-of-magnitude higher in fractured granite; however, the
 49 values depend on the precise geometry of the fractures at each site, and are thus not readily
 50 predictable in general. For example, Martinez-Landa and Carrera (2005) reported that in fractured
 51 granite at the Grimsel site K varies between $\sim 10^{-10}$ and $\sim 2 \times 10^{-8}$ m s⁻¹, with occasional more conductive

1 fractures. For fractured granite in Korea at depths of <100 m, Hamm et al. (2007) characterized the
2 statistics of variations of K , and how these correlate with length- and aperture-distributions of the
3 fractures; K here thus varies between $\sim 2 \times 10^{-10}$ and $\sim 3 \times 10^{-6} \text{ m s}^{-1}$. Illman et al. (2009) reported results
4 of tomographic analysis of pumping-test results to constrain variations in K in fractured granite in
5 Japan. Their results vary between $\sim 6 \times 10^{-8}$ and $\sim 10^{-6} \text{ m s}^{-1}$, the latter value occurring at ~ 500 m depth.
6 Since fractures in granite (and other rocks) are typically created as a result of the effects of cooling
7 and erosional unloading (cf. Brace et al., 1968; McGarr and Gay, 1978; Bourne and Willemse, 2001),
8 one expects them to open progressively as depth decreases. Furthermore, since permeability and
9 hydraulic conductivity depend on the cube of fracture aperture (e.g., Snow, 1969), one expects these
10 quantities to decrease with increasing depth. However, it is difficult to extrapolate results such as
11 those stated above for the higher pressure at greater depths. Overall, one does not expect K to be low
12 enough at depths of ~ 2000 m in granite to sustain hdDGSW operation, although exceptions (at the
13 high- K 'tail' of probability distributions) occasionally occur.

14
15 To illustrate this point with UK examples, Table 3 lists analyses of the hydraulic transport properties
16 for the Rosemanowes production well (well RH-15) in the Carnmenellis granite, Cornwall (after
17 Richards et al., 1994), and for the Eastgate-1 borehole in the Weardale granite, County Durham (after
18 Manning et al., 2007, and Younger and Manning, 2010). Well RH-15 only has sufficient hydraulic
19 conductivity to be viable as a hdDGSW over restricted vertical extents, none of which has sufficient
20 transmissivity to yield the required flow. Furthermore, the transmissivity and conductivity values are
21 relative to a nearby injection well; if that had not been operating, no fluid would have been produced
22 at this production well. At Eastgate, rapid ingress of water occurred at ~ 410 m depth when the
23 wellbore crossed a mineral vein, revealing the highest transmissivity ever measured within granite
24 (Younger and Manning, 2010). Setting aside this exceptional discovery, the water ingress into the rest
25 of this borehole at first sight indicates sufficient transmissivity for its use as a hdDGSW. However, as
26 Manning et al. (2007) pointed out, this ingress occurs at points where the wellbore crosses other
27 fractures, the most important of these being at ~ 730 and ~ 756 m depths. Once again, the
28 overwhelming majority of the section in this borehole evidently has very low hydraulic conductivity,
29 making it unsuited for use as a hdDGSW. The flow rates in the highly transmissive parts of this borehole
30 are far in excess of what would be needed for hdDGSW operation; as Manning et al. (2007) and Atkins
31 (2013) indeed noted, they might indeed be utilised for a conventional well doublet.

32
33 An additional factor affecting the viability of any dDGSW system, evident from previous analyses of
34 shallow systems (e.g., Rees et al., 2004), is the increase in operating costs that will result from the
35 greater drawdown within the borehole, which will accompany increased rates of 'bleed flow', due to
36 the need for pumping to lift the circulating water through a greater height. If significant 'head lift' for
37 produced water is necessary, the electrical power requirement might be large (e.g., Younger, 2014),
38 potentially outweighing the value of the heat produced. To analyse this effect, q_C and q_B may be
39 designated, respectively, as the volume flow rate required to produce heat by conduction (i.e., for the
40 closed-loop circulation within a DGSW borehole heat exchanger) and the rate of bleed flow, with
41 $\Gamma \equiv q_B/q_C$. It is assumed that the heat production utilizes a heat pump with coefficient of performance
42 (COP; the ratio of useable heat output to electrical energy consumed) Ψ , the heat is sold at a price P_H
43 per unit of energy produced, and the electricity used to power the heat pump contributes its own
44 heating effect, then the rate of heat sale can be expressed as $\rho \times c \times \Delta T \times (q_C + q_B) \times ((\Psi + 1)/\Psi) \times P_H$ where ρ
45 and c are the density and specific heat capacity of the circulating water and ΔT is its temperature
46 above ambient. The rate of expenditure on operating costs can be expressed as $\rho \times g \times H \times (q_C + q_B) \times P_E +$
47 $\rho \times c \times \Delta T \times (q_C + q_B) \times (1/\Psi) \times P_E$ where g is the acceleration due to gravity, H is the lift height or 'hydraulic
48 head' in the borehole, and P_E is the cost per unit of electrical energy used. The first of these terms
49 represents the 'head lift' pumping and the second the operation of the heat pump, both these
50 processes being assumed 100% efficient. Defining $\beta \equiv P_E/P_C$, the difference in operating surplus (or
51 deficit) between using bleed flow and omitting it from the design (thus assuming a closed loop

1 configuration with $H=0$, and with $\Gamma=0$) can thus be determined. The condition for the alternative open
 2 loop design (with H and γ both nonzero) being the more profitable of the two can thus be written,
 3 after several algebraic steps, as $H < H_0$ where

$$4 \quad H_0 = \frac{c \Delta T}{g} \frac{\Gamma}{1 + \Gamma} \frac{1 + \Psi - \beta}{\Psi \beta} . \quad (22)$$

7 Using plausible values for these parameters ($\Delta T=40$ °C, $c=4186$ J kg⁻¹ °C⁻¹, $g=9.81$ m s⁻², $\beta=3$ and $\Psi=4$),
 8 H_0 is ~250 m for $\Gamma=0.1$, increasing to ~1400 m for $\Gamma=1$. As another example, Law et al. (2015) discussed
 9 a dDGSW scenario in which 200 kW of heat production at $\Delta T=40$ °C was inferred to include a
 10 contribution of 50 kW from bleed flow. Thus, $\Gamma=1/3$, $q_c \sim 0.9$ l s⁻¹ and $q_b \sim 0.3$ l s⁻¹ are required. From
 11 equation (22), H_0 is ~700 m; equating this value to ΔH_0 in equation (21) gives $K \sim 9 \times 10^{-10}$ m s⁻¹. Even
 12 with such extreme drawdown, it is unlikely that K will be low enough in intact granite to make dDGSW
 13 operation worthwhile; moreover, this calculation takes no account of capital cost, which might make
 14 neither the cDGSW nor the dDGSW option economic relative to other energy sources (see below).

16 *Produced water treatment and associated costs*

17 As already noted, it is a legal requirement in the UK (and other European Union member states) for
 18 produced water discharged into the environment from boreholes to comply with regulatory limits for
 19 concentrations of contaminants such as dissolved metallic ions, and if necessary to require treatment
 20 (e.g., DEFRA, 2014). From previous experience (e.g., Edmunds, 1975, 1986; Younger et al., 2016),
 21 water produced from depths of ~2 km or more is expected to be a concentrated brine, potentially
 22 containing dissolved metallic ions including radionuclides in significant concentrations. Radium, an
 23 example radionuclide, is chemically similar to calcium, so can precipitate as radioactive scale within
 24 pipework, thus requiring costly treatment. Setting the latter aspect aside for now and concentrating
 25 on the discharge of produced water, treatment technologies are classified as active or passive (e.g.,
 26 Johnson and Hallberg, 2005): the former typically require inputs of electricity and chemical reactants,
 27 making them more expensive; the latter typically involve 'natural' processes such as filtration and
 28 biochemical reactions (e.g., sulphate reducing bacteria removing metallic ions from solution as
 29 insoluble sulphide 'sludge'), which typically proceed without routine human intervention within
 30 artificial wetlands at site. Active treatment options include installing treatment plant at site or
 31 transporting produced water by tanker lorry for treatment elsewhere. There is a substantial literature
 32 on this topic; contributions relevant to UK issues include the works by Younger (2000) and Younger et
 33 al. (2002, 2005). Many workers (e.g., Kiessig et al., 2004; Younger et al., 2005) have noted that cost
 34 estimates depend on site-specific details, including discharge rates, so once again 'off the shelf'
 35 solutions are not possible. It should also be noted that rather than preventing all pollution from
 36 entering the environment, the aim of these treatment options is to reduce pollutant concentrations
 37 to 'acceptable' levels that the environment can bear (e.g., Kiessig et al., 2004); adopted strategies thus
 38 require regulatory approval.

40 Since hdDGSW installation in granite is being proposed (GEL et al., 2016; Collins and Law, 2017; see
 41 below), the track record of treatment of mine water discharges from this lithology is relevant. The
 42 largest mine water treatment scheme in a granitic region of the UK is for the former Wheal Jane tin
 43 and copper mine in Cornwall, SW England (e.g., Knight Piesold and partners, 1995, 1998; Coulton et
 44 al., 2003; Younger et al., 2005), which adjoins the Variscan age Carnmenellis pluton. Commissioned in
 45 the 1990s, this active treatment scheme was originally budgeted with £4.25M capital cost and £1.03M
 46 annual operating cost, to treat ~5×10⁶ m³ of water per year (e.g., Knight Piesold and partners, 1998)
 47 at a typical rate of ~160 litres per second, principally for removal of iron, copper and zinc, also arsenic,
 48 cadmium, manganese, nickel and aluminium. The annual operating cost has subsequently been
 49 reported as ~£1.5M (e.g., Morris, 2014; Peacock, 2014), or ~£0.3 per cubic metre.

1 Bailey et al. (2016) describe a more recent active treatment scheme, to remove zinc from discharge
2 from the former lead and zinc mine at Force Crag in Cumbria, NW England, a region underlain by
3 Caledonian age granite plutons. Bailey et al. (2016) reported that the option chosen had a capital cost
4 of €1.92M and annual operating cost of €0.17M to treat discharge at $\sim 6 \text{ l s}^{-1}$. The latter amount is
5 $\sim \text{€}0.9$ or $\sim \text{€}0.8$ per cubic metre. Alternative passive treatment options would have been cheaper, but
6 were not preferred because of the proven technology adopted (Bailey et al., 2016).

7
8 For comparison, passive treatment is utilized for example at the former Pöhla-Tellerhäuser uranium
9 mine in the Erzgebirge mountains of SE Germany. Uraniferous mineralization occurs here in
10 hydrothermal veins associated with Variscan granite intrusions (e.g., Förster, 1999; Förster et al.,
11 1999). As discussed, for example, by Kunze and Kuchler (2003), Kiessig et al. (2004) and Kuchler et al.
12 (2005), after uranium mining ceased in 1990 the main concerns at this site have been dissolved iron,
13 radium and arsenic, as well as uranium and manganese, in waters that discharge at $\sim 17 \text{ m}^3 \text{ hr}^{-1}$ or
14 $\sim 5 \text{ l s}^{-1}$. The passive treatment system, installed at a capital cost of $\sim \text{€}0.5\text{M}$, comprises six artificial
15 wetlands covering almost 500 m^2 of land. The operating cost was estimated as $\sim \text{€}2$ per cubic metre in
16 the first two years of operation, when its performance was intensively monitored, subsequently
17 decreasing to $\sim \text{€}0.2$ or $\text{€}0.17$ per cubic metre. This system superseded an active treatment plant with
18 operating cost $\sim \text{€}4$ per cubic metre; it paid for itself in circa one year.

19
20 Turning to the possible option of transporting produced water for off-site treatment, it is noted that
21 the 2 l s^{-1} discharge rate envisaged for a dDGSW would result in 173 m^3 of produced water per day.
22 Transporting this volume to a treatment plant in 20 m^3 tanker lorries would require 9 movements
23 every 24 hours. The cost of treatment depends on local conditions and potential economies of scale;
24 Dahm and Chapman (2014) reported that in the USA such costs might thus vary between 0.20 and
25 8.50 per barrel ($\sim \text{€}1\text{-€}40$ per cubic metre). As Collins (2016) has discussed, in the USA water treatment,
26 including transportation by tanker lorry, for a small-scale installation such as this might cost 2.80 per
27 barrel, equivalent to $\sim \text{€}9$ per cubic metre or $\sim \text{€}1600$ per day. One might break this amount down in
28 terms of the costs of buying and operating the tanker lorries required, the wages for their drivers, and
29 the direct costs of the water treatment, using whichever technology is adopted at the treatment site.
30 Dahm and Chapman (2014) also described modular active treatment units, which can operate
31 automatically at drilling sites without routine operator intervention, and might (subject to
32 environmental permitting) discharge the treated water directly into the environment (e.g., into the
33 sea). The treatment cost was reported as ~ 0.75 per barrel or $\sim \text{€}3.80$ per cubic metre. Each of these
34 calculations assumes continuous operation, whereas a dDGSW might be operated intermittently, at
35 times of peak heat demand. Such intermittency would result in higher unit costs for treatment of
36 produced water, because assets (e.g., tanker lorries) would only see intermittent use.

37
38 It is evident that these costs require consideration relative to the value of the heat that is produced.
39 For example, if a dDGSW or hdDGSW produces heat at 400 kW with 2 l s^{-1} of 'bleed flow', it implies
40 18 litres of discharge per kWh. If the water treatment costs as much as $\text{€}3.80$ per cubic metre (see
41 above), it would equate to $\text{€}0.068$ per kWh. If each kWh of heat produced has a notional value of, say,
42 $\text{€}0.03$, then the water treatment cost would exceed the value of the heat produced, calling the
43 economics of the project into question. This is of course not a definitive limit as the value of the heat
44 produced might be influenced by subsidy payments (see below). Nonetheless, even if cheaper water
45 treatment is feasible, its cost might well be a substantial proportion of the value of the heat produced
46 and thus form an essential budget component for any project.

47 48 **Analysis of hcDGSW economics**

49 The preceding sections highlight several difficulties with the DGSW concept. First, dDGSW or hdDGSW
50 operation requires rocks of relatively high hydraulic conductivity at depth. Second, treatment costs
51 for the produced water will adversely impact economic viability, making dDGSW or hdDGSW

1 operation particularly problematic in granite; intact granite will have too low a hydraulic conductivity
2 and even if the granite is fractured the probability of a given section in it of vertical extent ~100-300 m
3 having sufficient transmissivity is low. Whilst one might conceivably find a suitable site for this
4 technology somewhere, it would require a substantial research (e.g., using electrical prospecting
5 techniques; cf. Beamish, 1990), thus defeating the aim of providing an 'off the shelf' technology. The
6 third issue concerns the cDGSW variant. In its simplest form, without a heat pump (Fig. 2(a)), the COP
7 will be high; for example, Law (2014) reported that a prototype installation had a COP of ~50.
8 However, as already noted, T_D for this variant will significantly exceed the ambient temperature T_S so
9 f will be well above zero, limiting the useable heat output. In contrast, for the hcDGSW variant, with
10 the circulating fluid also fed through a heat pump, to reduce its reinjection temperature much closer
11 to T_S (Fig. 2(b)), significantly higher heat production can be anticipated, in accordance with earlier
12 discussion, outweighing the fact that the COP for the additional heat output supplied via the heat
13 pump will inevitably be less than that extracted via the heat exchanger (see below). On this basis, the
14 hcDGSW is the variant with the greatest potential viability.

15
16 A model is thus developed to assess the output performance and economics of a hcDGSW. It is
17 assumed that an electrically powered pump maintains the circulation around the closed loop at the
18 rate necessary for the required rate of heat production by creating a pressure difference ΔP . ΔP will
19 equal the sum of pressure drops along the circulation loop, in the heat exchanger and the associated
20 pipework. Most of this pressure drop will be in the pipe carrying the upward component of the
21 circulation, as a result of its substantial length L and relatively small diameter D . Neglecting other
22 contributions, one may write (e.g., from Lyons et al., 2009, p. 167)

$$23 \quad \Delta P = \frac{f_D \rho V^2}{2 D} L \quad (23)$$

24 where f_D is the Darcy-Weisbach friction factor for the flow regime. The value of f_D itself depends on
25 the Reynolds Number, Re , of the flow, where

$$26 \quad Re \equiv \frac{V D \rho}{\eta} \quad (24)$$

27 η being the (dynamic) viscosity of the fluid. In general, if $Re < \sim 2000$, the flow is laminar, whereas at
28 higher Re it is turbulent. For laminar flow, f_D takes standard values as a function of Re (e.g., McKeon
29 et al., 2004). However, for turbulent flow, f_D also depends strongly on the roughness, Ω , of the inner
30 surface of the pipe, being markedly higher the rougher this is. Ω is defined as

$$31 \quad \Omega \equiv \frac{\varepsilon}{D}, \quad (25)$$

32 where ε is the characteristic height of surface irregularities; ε might be ~0.05 mm for steel pipe or
33 ~0.005 mm for composite or plastic pipe (e.g., Enggcyclopedia, 2011). One may look up f_D for the value
34 of Ω corresponding to any choice of ε and D and for any given value of Re on a standard 'Moody
35 Diagram' (Moody, 1944) for input into calculations using equation (23).

36 Assuming 100% efficiency, the electrical power Q_E used by the pump will equal $\Delta P \times Q$; assuming, also,
37 that all the produced heat is used, the COP, Ψ , will equate to Q / Q_E . These equations can be combined
38 to give

$$39 \quad \Psi = \frac{\pi^2 \rho^2 c^3 (T_O - T_S)^3 D^5}{8 f L Q^2} \quad (26)$$

40 As a test of this equation, it is noted, once again, that Law (2014) reported $\Psi \sim 50$ for a prototype
41 cDGSW installation, which had instantaneous heat production $Q=380$ kW, $L=1800$ m, and $T_O=63$ °C. T_S
42 can be estimated as ~10 °C and ρ , c and η as ~1000 kg m⁻³, ~4186 J kg⁻¹ °C⁻¹, and ~0.45 mPa s,

1 respectively, so q_B was $\sim 1.7 \text{ l s}^{-1}$ but D was not specified. Westaway (2016) estimated D as ~ 40 mm
 2 from a photograph of the pipe used in this prototype test, which implies $V \sim 1.4 \text{ m s}^{-1}$, suggesting Re
 3 $\sim 120,000$. The flow was thus highly turbulent; from Moody (1944) for very smooth pipe f_D would be
 4 ~ 0.018 . For this configuration, equation (26) predicts $\Psi \sim 300$, although with $D \sim 30$ mm it would reduce
 5 to ~ 70 , in rough agreement with the Law (2014) estimate. The ‘thermosiphon effect’, whereby the
 6 lower mean density of the fluid in the inner pipe, due to its higher mean temperature, reduces the
 7 pressure drop below the value of ΔP calculated using equation (23), and thus reduces the electrical
 8 power requirement for pumping (e.g., Alimonti et al., 2016; Spitler et al., 2016) and the associated
 9 operating cost, is also neglected; the calculations set out below indicate that this item forms a minimal
 10 part of the overall budget of a DGSW project.

11
 12 The COP for the heat pump, when extracting heat from a source at temperature T to a heat load at
 13 temperature T_E , is assumed to vary, after Baster (2011), as

$$14 \quad \Psi = 6.70 \exp(-0.022 \times (T_E - T)) \quad . \quad (27)$$

15
 16
 17 If the heat pump thus cools the circulating fluid from an initial temperature T_i to the ambient surface
 18 temperature T_s , its mean COP, Ψ_M , will be

$$19 \quad \Psi_M = \frac{1}{T_i - T_s} \int_{T_i}^{T_s} \Psi \, dT \quad (28)$$

20
 21 or

$$22 \quad \Psi_M = \frac{6.70}{0.022 (T_i - T_s)} \left(\exp(-0.022 \times (T_E - T_i)) - \exp(-0.022 \times (T_E - T_s)) \right) \quad . \quad (29)$$

23
 24
 25
 26
 27 The heat exchanger is presumed to cool the circulating fluid to temperature T_E ; the heat pump then
 28 cools it further, from T_E to T_s , after which it is reinjected. If $T_0 < T_E$ then the heat exchanger is assumed
 29 to be bypassed, such that $T_i = T_0$. Equation (27), for heat pump performance, was derived by Baster
 30 (2011) by regression analysis using an ensemble of performance data for air source heat pumps. It is
 31 used here as an approximation, in the absence of performance data for any water source heat pump
 32 with the required operating characteristics. The analysis proceeds by calculating the variation of T_0
 33 with time for a given Q using equations (3), (4) and (5), then calculating the heat outputs from the
 34 heat exchanger and heat pump, along with their electricity consumption. The calculations are run for
 35 a lifespan of 20 years consistent with the current RHI subsidy regime.

36
 37 Recent geothermal projects in the UK have involved drilling to ~ 1 km at Eastgate, County Durham
 38 (Manning et al., 2007; Younger and Manning, 2010), with a budget of $\sim \text{£}0.5\text{M}$, and to ~ 1.8 km at the
 39 Science Central site in Newcastle upon Tyne (e.g., Westaway and Younger, 2016; Younger et al., 2016),
 40 with a budget of $\sim \text{£}1.2\text{M}$. The $\text{£}1.35\text{M}$ capital cost estimated by GEL et al. (2016) for the proposed
 41 2 km AECC borehole is consistent with these values. In the geothermal project costing model used in
 42 the Netherlands, boreholes of depth z_M (in metres) have estimated capital cost Σ (in €)

$$43 \quad \Sigma = f_k (0.2 \times z_m^2 + 700 \times z_M + 250000) \quad (30)$$

44
 45
 46 (van Wees et al., 2010), where f_k is a scale factor to incorporate overheads, typically set to 1.5. This
 47 predicts much higher costs than would be expected in the UK, reflecting different local conditions
 48 (salaries, etc). However, it can be used to estimate the costs of deeper onshore boreholes in the UK,
 49 none having been drilled for many years, in proportion to the cost of drilling to 2000 m. One can thus
 50 estimate $\text{£}1.80\text{M}$, $\text{£}2.28\text{M}$ and $\text{£}3.44\text{M}$ as the capital costs of 2500 m, 3000 m and 4000 m boreholes,
 51 $\sim 33\%$, $\sim 69\%$ and $\sim 155\%$ higher, respectively. Again for the AECC project, GEL et al. (2016) have

1 estimated a budget of £2.293M, consisting of £1.350M for drilling and completion of the well,
 2 £0.265M for the required equipment, and £0.678M for overheads, including project planning and
 3 project management costs. The ‘off the shelf’ nature of hcDGSW schemes is expected to reduce
 4 planning and project management costs; such a project based on a 2 km borehole might thus be
 5 delivered for well below £2M, say ~£1.8M, with corresponding costs estimated as ~£2.4M, ~£3.0M
 6 and ~£4.6M for 2.5 km, 3 km or 4 km boreholes. It is assumed that the electricity used costs £0.095
 7 per kWh, a typical tariff for a ‘large’ industrial consumer in the UK (DECC, 2016a), the heat produced
 8 is sold at £0.03 per kWh, and a RHI subsidy of £0.0514 per kWh is payable. Once the system is
 9 commissioned, it is assumed to operate automatically, so the operating costs equate to the cost of
 10 the electricity used.

11
 12 Figure 7(a) illustrates the predicted revenue surplus (revenue, including RHI subsidy payments, minus
 13 operating costs) over a 20 year project lifespan for the 2000 m hcDGSW installation. The optimum
 14 configuration has $Q=193$ kW and yields a revenue surplus of £2.44M. Figures 7(b) and (c) illustrate the
 15 corresponding solutions for $z_M=2500$ m, with the optimum at $Q=295$ kW, yielding a revenue surplus of
 16 £3.71M; $z_M=3000$ m, with the optimum at $Q=416$ kW, yielding a revenue surplus of £5.23M; and
 17 $z_M=4000$ m, with the optimum at $Q=711$ kW, yielding a revenue surplus of £8.97M. It is thus evident
 18 that with optimal operation each of these designs can cover its own capital cost, the budget surplus
 19 increasing with z_M . More formal economic calculations, for example calculating the Net Present Value
 20 at the end of the project life including index-linking, to take account of future price inflation, of subsidy
 21 payments, heat sales, and estimates of future costs of electricity purchase, would reach similar
 22 conclusions. Figure 9 illustrates the predicted variations over time in T_0 for the four solutions in Fig.
 23 7. Overall, these calculations indicate that, over the depth range 2-4 km, the deeper a hcDGSW
 24 borehole is, the more heat it can produce on a given timescale, the value of the increased heat
 25 production outweighing the increased cost of drilling. The ensemble of solutions obtained for different
 26 depths z_M indicate that the optimum heat output and operating surplus over 20 years, Q and S , vary
 27 with z_M as:

28
 29
$$Q = 0.000131 z_M^{1.87} \tag{31}$$

30
 31 and

32
 33
$$S = 0.00000166 z_M^{1.87} \tag{32}$$

34
 35 with Q in kW and S in M£. Combining equations (31) and (32) gives

36
 37
$$S = 0.0127 Q \tag{33}$$

38
 39 indicating proportionality between S and Q , a surprising result given the complexity of the equations
 40 whose solution yields the values of S and Q .

41
 42 Once the twenty-year duration of the RHI subsidy has elapsed, continued heat production at what was
 43 previously the economically optimum rate would no longer be economic for $z_M=2000$ m, 2500 m, or
 44 3000 m, but would be economic for ~5 years longer for $z_M=4000$ m (Fig. 9). A possible next phase might
 45 be to re-purpose such a borehole for seasonal heat storage rather than heat production, as Westaway
 46 (2016) has discussed. Based on Westaway’s (2016) calculations, the rocks surrounding a 3000 m deep
 47 vertical borehole might have a seasonal heat storage capacity of ~2 GWh. Currently the RHI subsidy
 48 scheme excludes production of stored heat from any deep borehole, making it uneconomic in the UK
 49 to purpose-drill boreholes for this function. However, once the capital cost of a borehole has already
 50 been discounted as a result of heat production, it might thus be reused at little additional extra cost.
 51 Ultimately, after many such boreholes have been developed, such reuse might contribute significantly

1 towards achieving a sustainable provision of heat supply, which represents ~50% of the energy
2 demand in the UK (e.g., DECC, 2012).

3
4 The limited output of useable heat from hcDGSW projects invites economic comparison with other
5 small-scale renewable energy technologies, such as micro hydro schemes (cf. Bracken et al., 2014).
6 Bracken et al. (2014) indeed discussed one such scheme in northern England, with a capital cost of
7 £415,000, producing 0.165 GWh of electricity per year with an estimated 40 year lifespan, so 6.6 GWh
8 in total. Assuming the resulting zero-carbon output substitutes for electricity derived from the UK's
9 current generating mix (in 2015, 337.7 TWh of electricity was generated with 144.1 MT of CO₂e
10 emissions, according to DECC, 2016b, and BEIS, 2017, giving 0.427 kg CO₂e per kWh), the lifetime
11 carbon budget can be calculated. If the project began operating now (November 2017) its electricity
12 sales into the National Grid might attract a feed in tariff (FIT) of 7.78 p per kWh (OFGEM, 2017) in
13 addition to a sale price of maybe 5 p per kWh (e.g., Renewables First, 2015), so 12.78 p per kWh in
14 total. The total revenue from electricity sales over 40 years, at present prices, ~£843,000, would
15 significantly outweigh the capital cost, and would involve an overall saving in CO₂e emissions of 2818
16 tonnes. As a worst-case scenario, if a small part of the capital cost had been covered by a grant from
17 public funds, making the entire project ineligible for FIT subsidy, the revenue from electricity sales
18 would be only ~£330,000, making the net cost of the project at present prices ~£85,000, so the
19 emissions saving would have been achieved at a cost of ~£30 per tonne. However, DTI (1999)
20 estimated that the potential of micro hydro (and small-scale hydro) projects in the UK is ~35 TWh per
21 year, or roughly 10% of the present generating capacity (and, thus, ~2.5% of the total energy supply).
22 Thus, although this technology is economic under the present subsidy regime, it has insufficient
23 capacity to make a significant difference to the present-day energy mix.

24
25 The economically optimum $z_M=3000$ m hcDGSW solution in Fig. 7(c) and Fig. 9 produces 92.7 GWh of
26 heat and consumes 24.4 GWh of electricity over 20 years, at average annual rates of 4.64 and 1.22
27 GWh yr⁻¹. If the heat were used to offset burning of natural gas (with emissions equivalent to 0.181 kg
28 CO₂e per kWh according to EIA, 2016) and the electricity were again derived from the UK's current
29 generating mix, the lifetime carbon budget can be calculated. Allowing for the carbon embodied in
30 the construction of the hcDGSW (CO₂e of ~110 tonnes for the drilling activities and ~240 tonnes for
31 the materials used, assuming use of well-casing made of a corrosion-resistant composite material;
32 data from GEL et al., 2016, scaled in proportion to $z_M=3000$ m), the overall carbon budget (expressed
33 in terms of CO₂e emissions) balances a saving of ~16785 tonnes against ~10422 tonnes for the
34 electricity used plus the embodied ~350 tonnes, giving a net saving of ~6013 tonnes. The overall cost
35 of the RHI subsidy would be ~£4.77M, or ~£793 per tonne of CO₂e emissions saved. Calculated on the
36 same basis, the $z_M=4000$ m solution in Fig. 7(d) and Fig. 9 would produce 151 GWh of heat and
37 consume 34.7 GWh of electricity over 20 years, achieving a net saving of ~11995 tonnes of CO₂e
38 emissions in return for a RHI subsidy of ~£7.75M or ~£646 per tonne.

39
40 The above values can be compared with costs and environmental benefits of other energy supply
41 technologies (such as, micro hydro projects) or energy efficiency measures. The results indicate that
42 hcDGSW projects can be economic in a locality with a geothermal gradient as high as 32 °C km⁻¹. Table
43 4 lists the towns and cities in Britain where the geothermal gradient is as high as this. The urban areas
44 thus covered represent ~20% of the UK population, so the potential capacity of DGSW projects in
45 these localities might amount to ~20% of the demand for space heating or ~10% of the total energy
46 demand in the UK. Thus, although the cost per unit emission saving is much greater than for, say,
47 micro hydro, the overall potential of this technology is also much greater.

48
49 The cost per unit emission saving can be reduced significantly by operating a hcDGSW below its
50 economically optimum heat production rate. For example, for the aforementioned $z_M=3000$ m design,
51 operation for twenty years at $Q=215$ kW would consume 4.9 GWh of electricity at cost of ~£0.5M and

1 output 42.6 GWh of heat providing ~£3.5M of revenue, including RHI subsidy, thus just covering the
2 ~£3.0M capital cost, but reducing the cost per unit emission saving to ~£416 per tonne of CO_{2e}
3 emissions saved. Likewise, for the $z_M=4000$ m design, operation for twenty years at $Q=328$ kW would
4 consume 5.2 GWh of electricity costing ~£0.5M and output 62.7 GWh of heat providing ~£5.1M of
5 revenue, thus just covering the ~£4.6M capital cost, but further reducing the cost per unit emission
6 saving to ~£372 per tonne of CO_{2e} emissions saved. Anticipating future decarbonisation of electricity
7 generation, greater savings in emissions at correspondingly reduced unit cost would result. A future
8 regulatory regime might approve subsidy payments subject to a mode of operation that achieves an
9 approved compromise between the economically optimum and environmentally optimum heat
10 outputs. These economic and environmental considerations confirm that the hcDGSW concept might
11 have substantial potential as a source of low-carbon heat, warranting more detailed investigation.

12 **DGSW Case studies**

14 Arguably the most detailed published numerical model for a cDGSW is that by Alimonti and Soldo
15 (2016), which was applied by these authors and by Alimonti et al. (2016) to assess the geothermal
16 potential of repurposing a disused oil well at Villafortuna in northern Italy. Their analysis makes various
17 assumptions, for instance that the radius of the cooling effect around a cDGSW, given by equation
18 (12), is exact rather than an approximation. Their method, analyzing heat flow using the thermal
19 resistance of each concentric component of the borehole heat exchanger and surrounding rock
20 volume, is valid under steady-state conditions (e.g., Carslaw and Jaeger, 1959, pp. 189-193), and is
21 thus also an approximation under the non-steady-state conditions during DGSW operation.
22 Furthermore, as already noted, their analysis assumed operation at constant volume flow rate, with
23 heat production declining over time, rather than at a constant rate of heat production, although after
24 many years of operation their predicted rate of change of the rate of heat production is low.
25 Nonetheless, for the parameters applicable to their case study ($z_M=6100$ m, $a \sim 0.1$ m, and $D=0.045$ m
26 for the borehole; $T_S=25$ °C, $T_M=170$ °C, $k=2.5$ W m⁻¹ °C⁻¹, and $\kappa=1.2$ mm² s⁻¹ for the surrounding rock
27 volume; and $T_D=40$ °C for the surface heat exchanger installation) Alimonti et al. (2016) determined
28 that the optimum operational mode required $q_B=20$ m³ hr⁻¹, resulting in $Q=1200$ kW at $T_O=100$ °C after
29 10 years of operation. For comparison, using the present analytic model with the same input
30 parameters, $T_O=100$ °C after 10 years of operation would require output at a steady $Q=530$ kW.
31 However, it is unclear whether this means that the present analytic approach has a tendency to
32 underestimate the output achievable from cDGSW installations, or whether the difference in
33 operational mode or the approximations made in the Alimonti et al. (2016) analysis account for the
34 difference. Comparison will now be made between the results of the present analysis and the Law et
35 al. (2015) DGSW conceptual model. The economics of two proposed DGSW projects, in Aberdeen and
36 Kilmarnock, Scotland, and a hypothetical hcDGSW project in Darlington, northern England (cf. Table
37 4), will also be discussed.

38 *Law et al. (2015) conceptual model*

40 Law et al. (2015) presented numerical modelling results for a model DGSW operating in either cDGSW
41 or dDGSW modes. This was assumed to have z_M 2500 m, u 32 °C km⁻¹, and T_M 80 °C, implying $T_S=0$ °C;
42 other parameters (including T_L , a , k , and κ) were not specified. Law et al. (2015) stated that their
43 analysis used the U.S. Geological Survey finite element code SUTRA (Voss and Provost, 2010), their
44 mesh being defined for a volume of square cross-section with sides extending 250 m away from the
45 borehole, representing a single 90° quadrant (the other three quadrants being equivalent, given the
46 symmetry of the problem). They did not specify the spacing of elements within their mesh or indicate
47 the nature of the boundary conditions applied at its vertical and horizontal surfaces. Although SUTRA
48 is primarily intended for solving subsurface fluid flow problems, it can also calculate heat conduction
49 in the absence of fluid flow. As Law et al. (2015) explained, their method incorporates calculations
50 using the thermal resistance of each concentric component of the borehole heat exchanger and
51 surrounding rock volume. However, as already noted, this method is valid under steady-state

1 conditions (e.g., Carslaw and Jaeger, 1959, pp. 189-193), and thus serves only as an approximation
2 under the non-steady-state conditions that develop during DGSW operation.

3
4 The outputs of this model in cDGSW mode, for steady heat production of 50, 100, 200 and 400 kW,
5 over ten years of operation, are summarized in Fig. 4. Thus, after ten years, T_o is predicted to be ~70,
6 ~64, ~51 and ~27 °C, respectively, indicating cooling in each of these cases by ~10, ~16, ~29 and ~53 °C
7 at the bottom hole depth. The cooling on this timescale per kilowatt of heat production is thus ~0.20,
8 ~0.16, ~0.15, and ~0.13 °C kW⁻¹ for these four configurations. Their model is therefore non-linear,
9 despite the governing equations (e.g., equation (2)) being linear, which is difficult to understand. Law
10 et al. (2015) also inferred that for Q=50 or 100 kW their model cDGSW reaches a steady state within
11 ten years, which is untenable given that heat is being produced much faster than it is being replenished
12 by conduction from surrounding parts of the subsurface rock volume; however, this behaviour can be
13 described as an 'almost steady state condition' (see earlier discussion).

14
15 Although Fig. 4 indicates that the cooling curves predicted in the present study have similar general
16 shape to those reported by Law et al. (2015), they do not match closely, and cannot be made to agree
17 for any single set of model parameters. This latter aspect is illustrated in Fig. 8 in which the present
18 analytic solutions are converted into dimensionless form, using the dimensionless variables
19 $y = -4 \pi k \Delta T / q_M$ and $x = \ln(4 \kappa t / a^2)$. Transformed thus, these solutions all plot as the same straight
20 line with gradient -1 and y-intercept γ . However, when transformed in the same way, the Law et al.
21 (2015) solutions plot as curves, which do not overlie each other and diverge as x increases. Different
22 choices of the parameter values required to transform these solutions to dimensionless variables
23 would change the positions of these solutions on this plot but would not affect the predicted shape of
24 the transformed solutions, so incorrect choices of these values are not the cause of these mismatches.

25
26 It was initially assumed that the cause of these mismatches was the omission from the analytic model,
27 in its original form, of the borehole 'end-correction' and the effect of geothermal heat flow; hence,
28 the derivation of these corrections. It was indeed initially thought possible that these corrections
29 might have a larger effect the greater the subsurface cooling, and might thus act to 'draw in' additional
30 heat from the surroundings to the borehole, either below it or beyond it to the sides. However, the
31 small magnitude of these corrections (noted above), for DGSW operation over timescales relevant to
32 Figs. 4 and 8, mean that this is not the explanation.

33
34 It will be recalled that the calculations for cDGSW operation in the present study incorporate a balance
35 between heat production from the borehole heat exchanger and heat lost by conduction due to
36 cooling of the surrounding rock volume. It can also be presumed that the Law et al. (2015) calculations
37 likewise incorporate conservation of energy. Nonetheless, the Law et al. (2015) calculations indicate
38 less cooling of the rock volume surrounding the borehole at its bottom hole depth than the
39 calculations in the present study, despite indicating higher heat outputs. For this to be feasible while
40 maintaining conservation of energy requires the Law et al. (2015) numerical model to produce more
41 cooling than the present model across at least part of the range of depth between the Earth's surface
42 and the well bottom. The resulting creation of a non-linear geothermal gradient along the borehole
43 might account for the non-linear behaviour that has been noted. Nonetheless, the test data provided
44 by Law (2014) indicate a linear temperature gradient at depths where the temperature exceeds the
45 injection temperature T_D , and indeed motivated incorporating the equivalent assumption into the
46 present analytic model. However, these data only relate to eight hours of operation; in the absence
47 of test data documenting the DGSW behaviour on much longer timescales, this discrepancy cannot
48 currently be resolved.

1 The mismatch between predictions Q_A from the present analytic model and for Q_N from the Law et al.
2 (2015) and Alimonti et al. (2016) numerical models, for heat output rates over ten years of cDGSW
3 operation, is illustrated in Fig. 10. These data points fit the regression equation

$$4 \quad Q_N = 0.2995 Q_A^{1.3134} \quad (Q_A \geq 50 \text{ kW}) . \quad (34)$$

6
7 Calculations in the present study incorporate values of Q_A , but might in principle be modified to use
8 values of Q_N from this regression equation. This would result in significantly more favourable
9 assessments for options with $Q_A \gg 50$ kW. On the other hand, it is possible that the apparent
10 consistency between these two numerical modelling approaches might reflect their use of similar
11 methods, including applying theory for steady-state behaviour to non-steady-state situations, in which
12 case neither numerical method approach might provide accurate results.

13 *The HALO project, Kilmarnock*

14 Planning documentation (East Ayrshire, 2017) states that this project will produce heat at a rate of
15 2.1 GWh yr⁻¹, equivalent to a steady rate of 239 kW, from a 2 km deep borehole to be located at British
16 National Grid (BNG) reference NS 42641 38505. The geothermal gradient in this part of SW Scotland
17 can be estimated using data from the Slatehole borehole (British Geological Survey [BGS] identifier
18 NS42SE4; at NS 4907 2343, ~16 km to the SSE), where a bottom hole temperature of 40.0 °C at 1024 m
19 depth and a geothermal gradient of 29.8 °C km⁻¹ have been measured (e.g., Gillespie et al., 2013).
20 Extrapolation at a constant geothermal gradient would give a temperature of ~69 °C at 2 km depth.
21 The capital cost of this DGSW installation has been funded through a £1.8M grant from the Scottish
22 Government (Geon, 2017); as a result of this public funding of capital expenditure, the heat output is
23 ineligible for RHI subsidy. Law and Collins (2017) state that a heat pump would be used in any DGSW
24 installation with a basal temperature as low as this, given the need to interface with a heating system
25 operating at ~70 °C. Preliminary documentation (Geon, 2017) depicted a closed circulation loop,
26 implying (in the terminology used in the present study) that the design is for a hcDGSW. Subsequent
27 definitive documentation (East Ayrshire, 2017) indicates that the design will allow for the possibility
28 of bleed flow, but the standard operational mode will involve closed circulation; this project will
29 therefore be analysed as a hcDGSW. The same documentation (East Ayrshire, 2017) also indicates that
30 the design includes a very wide borehole, with a diameter of 0.75 m.

31
32
33 The reported output, equivalent to a steady 239 kW, is well above the optimum value of 194 kW for
34 a 2 km borehole under the high geothermal gradient conditions envisaged for Fig. 7(a), and is thus
35 likely to exceed even more the optimum operational mode for the lower geothermal gradient in the
36 Kilmarnock area. The local outcrop consists of the Scottish Coal Measures Group of Upper
37 Carboniferous (Westphalian) age, underlain by the Clackmannan Group (Namurian), Strathclyde
38 Group (Viséan), Inverclyde Group (Tournaisian), and Stratheden Group (Late Devonian). Like
39 elsewhere in Britain (cf. Westaway and Younger, 2016) such Carboniferous sequences consist of cyclic
40 alternations of lithologies (mudstone, sandstone, limestone, and coal) with diverse thermal
41 properties. For example, Carboniferous sandstone may have k as high as 4.9 W m⁻¹ °C⁻¹ (England et al.,
42 1980) whereas the value of k for coal will be an order-of-magnitude less (e.g., Westaway and Younger,
43 2016). The underlying Devonian 'Old Red Sandstone' rocks include tight sandstones for which k as high
44 as 5.2 W m⁻¹ °C⁻¹ has been measured elsewhere in Europe (Chekhonin et al., 2012). The thermal
45 conductivity and diffusivity applicable for the HALO DGSW will be a harmonic mean of the values for
46 these diverse lithologies in representative proportions, and has not been reported. Values of
47 $k=4$ W m⁻¹ °C⁻¹ and $\kappa=1.5$ mm² s⁻¹ will be assumed for the present analysis, although these might well
48 be overestimates; moreover, the high k in the deeper part of the section implies a lower geothermal
49 gradient than has been assumed by extrapolation from the Slatehole borehole dataset, suggesting
50 that the 69 °C bottom-hole temperature is probably also overestimated. This combination of

1 optimistic assumptions has been made to avoid any risk of underestimating the potential of the HALO
2 project, for the quantitative assessment that follows.

3
4 Figure 11(a) indicates that if heat were to be produced from the HALO DGSW at a steady rate of
5 239 kW, the output temperature would rapidly decline from the initial 69 °C, falling to ~23 °C over
6 twenty years. Figure 11(b) depicts the economic analysis of this DGSW for a 20 year assumed lifespan.
7 The economically optimum heat production rate is surprisingly low, ~32.4 kW, despite the optimistic
8 assumptions. This value is highly sensitive to the assumed pricing structures for heat and for electricity,
9 it being evident that the modest budget surplus depicted is due to the very small difference calculated
10 between expenditure on electricity and revenue from heat sales. A less favourable pricing structure,
11 or a lower bottom hole temperature (<58.1 °C), would make operation of this DGSW uneconomic
12 relative to the option of shutting it down and using the electricity saved (by not powering its heat
13 pump) to heat buildings directly. The economics of this project are indeed hampered by the output
14 temperature being always below the assumed 70 °C input temperature of the heat load (after Collins
15 and Law, 2017), so all the heat output has to be transferred through the heat pump, ~13.6 kW of
16 electrical power being required to supplement the ~32.4 kW of heat production to produce an overall
17 output of ~46 kW of useable heat. As Fig. 11(a) shows, with such a low rate of heat production, very
18 little temperature fall occurs within the DGSW over 20 years, so in principle this project could function
19 at this very low rate for a very long time.

20
21 Figure 12 shows the equivalent outputs for a project with the same design parameters as for HALO,
22 but with the borehole diameter reduced to 0.2 m. With this narrower borehole, if heat were to be
23 produced at a steady 239 kW, the output temperature would fall more rapidly, reaching ~23 °C within
24 eighteen months and ~11 °C after twenty years. However, the economically optimum heat production
25 rate, ~29.3 kW, producing ~41.5 kW of useable heat, does not differ much compared with the wider-
26 borehole design adopted. Given the lower capital cost and lower CO₂ emissions from drilling, which
27 would result from this alternative narrower-borehole design, the appropriateness of the proposed
28 design is called into question.

29
30 Overall, this HALO case study provides a graphic demonstration of the need to make DGSW
31 evaluations site specific, taking account of local thermal regime and mode of operation (cf. Law et al.,
32 2015; Collins and Law, 2017), the critical factor being accurate estimation of the initial bottom hole
33 temperature. Nonetheless, such calculations are much less challenging than the analysis of hydraulic
34 transport properties and groundwater contamination that would be required, from earlier discussion,
35 to quantify the output and economics of a dDGSW.

36 37 *Aberdeen Exhibition and Conference Centre*

38 A candidate hdDGSW project has been proposed for the Aberdeen Exhibition and Conference Centre
39 (AECC) in the Scottish city of Aberdeen (GEL et al., 2016), a ~2 km deep borehole being envisaged (to
40 be located circa BNG reference NJ 884 105), with a bottom hole temperature estimated by GEL et al.
41 (2016) as ~70 °C. It has been proposed that heat will be extracted via a heat exchanger to maintain
42 the temperature of an anaerobic digester (AD) for processing municipal waste, then the residual heat
43 (below T_E ~40 °C) will be output via heat pumps for space-heating in adjacent buildings, before the
44 circulating water is reinjected. The project description mentions system design to facilitate 'bleed
45 flow', the proposal specifying the bottom 300 m of the borehole uncased; given the preceding
46 calculations it is evident that the high heat output envisaged (up to 400 kW) will only be feasible with
47 bleed flow. Moreover, since the design calls for the AD unit to operate continuously, the proposal
48 envisages continuous (or near-continuous) bleed flow to sustain its operation.

49
50 The draft budget (GEL et al., 2016) indicates a ~£1.6M capital cost, ~£1.35M for the borehole, the rest
51 for the ancillary equipment. Estimated annual operating costs would be ~£49k and annual revenue

1 based on sale of heat at £0.03 per kWh would be ~£239k. On this basis the project has been reported
2 as achieving a high net present value of ~£10.7M after 40 years with a high internal rate of return of
3 ~19%; these economic parameters, which favour commercial investment, assume that RHI subsidy
4 payments (currently £0.0514 per kWh) are included. However, this analysis does not include water
5 treatment costs on the basis that 'as the Aberdeen granite is rather deficient in heavy metals it is very
6 unlikely that any fluids from the DGSW will be the cause of significant environmental contamination
7 by heavy metals', although no quantitative data were provided to substantiate this assertion.

8
9 Nonetheless, the surface heat flow in this part of Scotland is low, being depicted on BGS maps (e.g.,
10 Busby et al., 2011) as ~50 mW m⁻². Some 50 km to the SSW, the Montrose (or Charleton-1) borehole
11 (BGS identifier NO76SW12, circa BNG reference NO 715 605) has yielded a heat flow of 46 mW m⁻²
12 based on measurements of temperature and thermal conductivity k between 301 and 751 m depths
13 (e.g., Burley et al., 1984; Rollin, 1995); the ~20 °C temperature at 500 m depth indicates a geothermal
14 gradient u of ~22.8 °C km⁻¹, given the ~8.6 °C annual mean surface temperature (e.g., Met Office,
15 2017), which would imply ~54 °C at 2 km depth. However, ~7 km east of the AECC site, the Bridge of
16 Don-3 borehole (BGS identifier NJ91SE3, circa NJ 951 109) was drilled in basement schist to 1465 m
17 (TVD; 1494 m MD) but is now cased to 1433 m for use as a test facility by the oilfield service provider
18 Weatherford. The bottom hole temperature is reported as 32 °C (Groves et al., 2012), indicating u
19 ~16.3 °C km⁻¹, which would imply ~41 °C at 2 km. However, this measurement was made during drilling
20 and thus requires correction for the associated cooling effect. Established correction procedures exist
21 (e.g., Manetti, 1973; Barelli and Palama, 1981); there is also UK experience, such as for the Eskdale-12
22 borehole (BGS identifier NZ80NE4, NZ 85783 08180) in northern England, drilled in 1963 to 1873 m
23 depth, within which temperature was measured one hour after drilling and later, so the calculated
24 correction could be verified (Burley et al., 1984). Taking all this into account, it is estimated that the
25 Bridge of Don-3 measurement requires upward revision by ~15 °C at most, making u ≤26.2 °C km⁻¹ and
26 the temperature at 2 km ≤61 °C. The Aberdeen granite has low radioactive heat production: McCay
27 (2016) has reported 11 measurements spanning 1.55 to 3.11 μW m⁻³, with a mean of 2.17 and a
28 median of 2.04 μW m⁻³, confirming the ~2.2 μW m⁻³ mean value reported by Wheildon and Rollin
29 (1986) from 3 measurements. Basement rocks like those beneath Aberdeen are typically assigned heat
30 production of ~2 μW m⁻³ (e.g., Wheildon and Rollin, 1986); the Aberdeen granite is therefore not
31 expected to create a significant local heat flow 'high' relative to the above values. Part of the rationale
32 behind the GEL et al. (2016) temperature estimate at 2 km depth was their best-estimate
33 measurement for k in the Aberdeen granite of 2.71 W m⁻¹ °C⁻¹, on which basis they converted the
34 reported heat flow of ~50 mW m⁻² back to u ~18.5 °C km⁻¹, giving ~46 °C at 2 km depth. However,
35 Caledonian age granite intrusions in Scotland and northern England typically have k ~3.1-3.5 W m⁻¹ °C⁻¹
36 (e.g., Wheildon and Rollin, 1986), which (calculating on the same basis) would imply rather lower
37 temperatures at depth. GEL et al. (2016) also argued that the heat flow data require correction for
38 palaeoclimate, citing Westaway and Younger (2013), as a basis for their ~70 °C temperature estimate
39 at 2 km depth. However, the Westaway and Younger (2013) analysis (see, e.g., their Fig. 3) indicates a
40 negligible correction to u for the Bridge of Don-3 borehole and a ~5 °C km⁻¹ upward correction for the
41 Montrose borehole. On the latter basis, if the thermal state of the Earth's crust is the same at the
42 AECC site as at Montrose, one might argue for a temperature as high as ~64 °C at 2 km depth, although
43 the Bridge of Don-3 evidence indicates less than this. The discussions earlier in the present study,
44 which demonstrate high sensitivity of DGSW output to crustal thermal regime, mean that
45 overestimation of the bottom hole temperature can have a fundamental impact on project economics.
46 Nonetheless, ≥70 °C is expected at 2 km depth elsewhere in the UK, in more radiothermal granites
47 (e.g., Lee, 1986) and in Mesozoic depocentres such as the Wessex and Lincolnshire basins of England
48 and the Larne Basin of Northern Ireland (e.g., Smith, 1986). It is thus worthwhile to pursue the
49 implications of the GEL et al. (2016) analysis, since DGSW-based project proposals for such localities
50 might emerge in future.

1 Assuming income of £0.0814 kWh⁻¹ the revenue reported by GEL et al. (2016) implies heat sales of
2 ~2.93 GWh per annum, equivalent to a constant rate of ~334 kW. This is so far above what might be
3 feasibly delivered from a cDGSW of the specified dimensions with the proposed T_E that 'bleed flow'
4 will be essential, as already noted. This scenario can be analysed to first order assuming that ~100 kW
5 of this heat supply might be obtained through heat conduction (based on the preceding calculations),
6 the rest being obtained by 'bleed flow'. Setting aside the question of accurate estimation of T_M, two
7 issues thus call this project into question: the required high hydraulic conductivity of the granite that
8 is presumed to provide the groundwater reservoir for this project; and the arguable need to factor in
9 treatment costs for this produced water. Assuming T_M=70 °C and that all the heat is utilized down to
10 T_S=10 °C, the required circulation rate including the bleed flow would be ~334 kW / (4186 kg m⁻³ ×
11 1000 kg m⁻³ × 60 °C) or ~1.3 l s⁻¹; ~0.9 l s⁻¹ of this would be 'bleed flow' and the parameter Γ would
12 take the value ~234/100 or ~2.34. If the AD heat exchanger rejects heat below T_E=40 °C then this
13 component of its heat supply will be ~334 kW × (70 °C – 40 °C) / (70 °C – 10 °C) or ~167 kW. Taking
14 ΔT as 70 °C – 10 °C = 60 °C, equation (22) indicates H_o ~3000 m, greater than the assumed borehole
15 depth. However, for 'head lift' to have only a minimal effect on the project budget, the drawdown
16 must be only a small proportion of this, say 5% or ~150 m.
17

18 As already noted, Law (2014) reported a high value of ~50 for the COP at a DGSW test site where the
19 produced water was reinjected. As has also already been noted, this is not necessarily so in dDGSW
20 mode; if significant 'head lift' for the produced water is necessary, the electrical energy requirement
21 might outweigh the value of the heat produced. The AECC project design evidently assumes zero or
22 minimal 'head lift', meaning that the groundwater reservoir at depth has been assumed to be under
23 hydrostatic equilibrium with the ground surface which, as already discussed, requires a very high
24 hydraulic conductivity in the granite. Negligible electrical energy would therefore be needed for
25 pumping the produced water against gravity, the cost of which is neglected in these first-order
26 calculations. It is thus inferred that most of the electrical power consumed will be used by the heat
27 pumps, whose COP, Ψ, will be much lower (say, 4). If these cool the circulating water to 10 °C the
28 additional ~167 kW heat loss will require ~167 kW × 1 / (Ψ – 1) or ~56 kW of electrical power.
29 Assuming once again that the electricity used costs £0.095 per kWh, this heat pump operation will
30 cost of ~£46k per annum, indeed consuming most of the ~£49k estimated operating budget. This is
31 evidently an approximate analysis, but it implies that, per day of operation, typically, ~80 m³ of
32 produced water (~0.9 l s⁻¹ × 24 hrs) will require treatment. If this costs ~£3.80 per cubic metre (see
33 above) it will imply an additional cost of ~£300 per day or ~£110k per annum. Even with this additional
34 budget item, then provided T_M is indeed ~70 °C, the project would still be predicted to make an annual
35 surplus of ~£80k (~£239k revenue – £49k operating costs – £110k water treatment costs), again with
36 the RHI subsidy included in the revenue, although the ~£1.6M budget surplus thus accumulated over
37 20 years of operation would barely cover the capital cost of the drilling. Nonetheless, like for the HALO
38 project, this calculated small surplus is the difference between much larger figures for revenue and
39 expenditure, so is sensitive to small changes in these. If the granite has insufficient hydraulic
40 conductivity to maintain the required 'bleed flow', or if significant 'head lift' pumping is required,
41 increasing the electricity consumption with no additional heat output, or if the bottom hole
42 temperature is significantly below 70 °C, this project might well not recover its own capital
43 expenditure and might even operate at a deficit, with revenue unable to cover operating costs.
44

45 *Hypothetical Darlington hcDGSW project*

46 Table 4 lists Darlington as the town with the highest temperature at 1 km depth in Britain. This is based
47 on evidence from the Brafferton-1 borehole (BGS identifier NZ22SE105, located at BNG reference NZ
48 28432 21493) drilled to 1987 m depth, ~6 km north of Darlington town centre, for which Busby et al.
49 (2011) reported a temperature of 54 °C at 1 km depth. Darlington is located within the Stainmore
50 Trough or Stainmore Basin, one of several sedimentary basins in northern England, which formed as
51 a result of crustal extension during the Early Carboniferous. The base of the Carboniferous succession

1 is reported, from seismic surveys, at ~5700 m depth in the Darlington area (Chadwick et al., 1995).
2 The Brafferton-1 borehole record remains commercially confidential and unpublished, but from the
3 regional context (e.g., Collier, 1991; Chadwick et al., 1995), including deep drilling elsewhere (Johnson
4 et al., 2011), the local Carboniferous succession can be inferred to consist mainly of mudstone with
5 interbedded sandstone, limestone, and coal seams. A similar succession farther north, beneath
6 Gateshead, has $k \sim 1.7 \text{ W m}^{-1} \text{ }^\circ\text{C}^{-1}$ and $\kappa \sim 0.9 \text{ mm}^2 \text{ s}^{-1}$ (Westaway and Younger, 2016); these values will
7 be adopted for the present analysis. With this value of k , and a surface temperature of $\sim 9 \text{ }^\circ\text{C}$ from
8 meteorological data, the $\sim 45 \text{ }^\circ\text{C km}^{-1}$ geothermal gradient implies $\sim 77 \text{ mW m}^{-2}$ of heat flow. Other
9 localities beyond the northern margin of the Stainmore Basin have much higher heat flow, due to heat
10 production in granite intrusions, but lower temperatures at depth due to the higher thermal
11 conductivity of the rock column (e.g., Busby et al., 2011). The borehole cost model in use (equation
12 (30)) gives the capital cost of a 6000 m deep borehole, reaching the base of this sedimentary
13 succession, as $\sim \text{£}8.6\text{M}$.

14
15 It is assumed that this hcDGSW scheme will form part of a future district heating scheme for the urban
16 area of Darlington. In Denmark, such schemes often take as their input water at a temperature as low
17 as $\sim 50 \text{ }^\circ\text{C}$ (DEA, 2017); they achieve satisfactory space heating using radiators rather larger than are
18 customary in the UK. Even lower input temperatures, as low as $\sim 35 \text{ }^\circ\text{C}$, are feasible if underfloor
19 heating is used (e.g., Joule, 2017), rather than radiators of any size. It is assumed that the hypothetical
20 Darlington district heating scheme will be designed on this basis, with $T_E = 35 \text{ }^\circ\text{C}$. It is also assumed that
21 heat is sold, RHI subsidy applies, and electricity purchased, all at the same rates as before. The
22 electricity purchased is again assumed to reflect the present UK generation mix and the heat output
23 is again assumed to substitute for burning natural gas.

24
25 Figure 13 illustrates results of analysis of this hcDGSW scheme, developed, costed, and operated for
26 20 years on this basis. The economically optimum operational mode (Fig. 13(b)) has $Q = 1095 \text{ kW}$. This
27 generates net revenue of $\text{£}14.4\text{M}$, including a surplus of $\text{£}5.8\text{M}$ after taking account of drilling costs,
28 outputting 211.9 GWh of heat and consuming 30.2 GWh of electricity, saving 24769 tonnes of CO_2e
29 emissions at a cost of $\text{£}440$ per tonne. The environmentally optimum operational mode has
30 $Q = 490 \text{ kW}$. This produces 89.1 GWh of heat output and consumes 3.1 GWh of electricity, saving 14098
31 tonnes of CO_2e emissions at a cost of $\text{£}325$ per tonne. The net revenue is $\text{£}7.0\text{M}$, indicating a shortfall
32 of $\text{£}1.6\text{M}$ relative to the drilling costs. Any rate of heat production between 23 and 1208 kW results in
33 a net saving of CO_2e emissions: below 23 kW, the emissions embodied in the borehole drilling and
34 completion are not recouped; whereas, above 1208 kW, T_o falls so low (Fig. 13(a)) that much of the
35 heat extraction is via the heat pump and the associated consumption of electricity is so high that the
36 emissions associated with its generation outweigh those saved by the production of geothermal heat.
37 Despite the higher geothermal gradient and bottom hole temperature, and the greater length of the
38 borehole heat exchanger, the economically optimum heat production rate of 1095 kW is not much
39 greater than for the configuration in Fig. 7(d)). The essential reason for this is the smaller values of k
40 and κ that have been assumed ($\sim 1.7 \text{ W m}^{-1} \text{ }^\circ\text{C}^{-1}$ and $\sim 0.9 \text{ mm}^2 \text{ s}^{-1}$ compared with $\sim 3.5 \text{ W m}^{-1} \text{ }^\circ\text{C}^{-1}$ and
41 $\sim 1.2 \text{ mm}^2 \text{ s}^{-1}$), reflecting the exponential dependence on k (cf. equation (9)). Nonetheless, once again,
42 the economically optimum output scenario lies very close to the maximum output feasible, again
43 demonstrating the need for careful calculations to determine this optimum mode. This exercise
44 nonetheless demonstrates that deployment of a hcDGSW in a locality of high geothermal gradient,
45 used in an optimal manner, can produce worthwhile savings in CO_2e emissions.

46 47 **Conclusions**

48 A critical appraisal of the DGSW concept has been presented, driven by the apparent contradiction
49 between the long-standing view (Rybach et al., 1992) that this technology has no potential, other than
50 for repurposing existing boreholes, and claims by commercial developers. The present simplified
51 analytical modelling, which approximates the operational state of a DGSW installation under real

1 conditions, enables some misconceptions about DGSW technology, which have emerged through
2 previous work, to be corrected. It is thus evident, first, that although a cDGSW or hcDGSW might look
3 like an enlarged version of a shallow borehole heat exchanger used for a conventional GSHP
4 installation (and the governing equations, such as equation (4) [cf. Banks, 2012], are similar), its
5 operational principles are different: conventional GSHP installations can function sustainably, whereas
6 a cDGSW or hcDGSW is instead a form of ‘heat mining’. Operation of a cDGSW will indeed not attain
7 a steady state over timescales of practical projects (i.e., timescales of decades); the associated ‘heat
8 mining’ will instead progressively cool an ever-widening volume of surrounding rock, although each
9 part of this rock volume will cool at ever-decreasing rates. The governing thermal physics is linear, the
10 cooling at any point on any particular timescale being proportional to the rate of heat production.
11 Second, when analysing a cDGSW one must distinguish between the heat produced (the heat that
12 reaches the surface) and useable heat output, given that a proportion of the heat production (this
13 proportion depending on the input temperature of the surface heat exchanger) will be reinjected as
14 the heat transfer fluid is circulated. Analysis of the potential of any DGSW installation thus requires
15 consideration of the site-specific combination of geological properties (such as thermal
16 conductivity/diffusivity and geothermal gradient) and mode of operation, not the geological
17 properties alone. The heat reinjected during operation of a cDGSW makes this a less favourable
18 technological variant compared with the hcDGSW, notwithstanding the lower overall COP of the latter
19 due to the electricity consumed by its heat pump. The electrical energy thus consumed will be
20 converted to heat, providing another reason why the heat output from the system (including its heat
21 pump) will differ from the heat produced from the borehole. Furthermore, the heat production from
22 DGSW boreholes is sensitive to the site-specific geological properties; DGSW design must therefore
23 consider such properties on a site-by-site basis, rather than assuming nominal values or that an
24 analysis for one site is applicable to another. Moreover, economically optimal operation of a hcDGSW
25 involves a rate of heat production that is close to the maximum that can be sustained over the lifetime
26 of a project. This means that if a project has been ‘under-engineered’ (i.e., its heat output capacity has
27 been overestimated, even by a small margin), the surrounding rock volume will cool so rapidly that
28 the actual lifetime of the project is significantly reduced. The environmentally optimum operational
29 mode (optimizing savings in CO₂e emissions) involves heat production at a lower rate than the
30 economically optimum mode (maximizing profit). If such projects are subsidized from public funds,
31 then a particular operational mode might be specified, maybe as a compromise between these
32 optima. Additional issues also affect dDGSW or hdDGSW installations. First, the produced water might
33 well require decontamination treatment, especially if the installation is in granite, which will add
34 significantly to operating costs and might cause regulatory difficulties. Second, these DGSW variants
35 can only function in rocks of relatively high permeability and hydraulic conductivity, and the cost of
36 pumping to maintain ‘head lift’ can further impact upon the economics of operation.

37
38 The present analytic modelling, which approximates the operational state of a DGSW installation
39 under real conditions, indicates that the cDGSW variant has only limited potential; for 2 km deep
40 boreholes, outputs over 20 year timescales of at most ~100 kW are feasible, the value of which (under
41 current UK conditions) is unlikely to cover the capital costs. hdDGSW operation can produce higher
42 heat outputs, and can in principle be economic under current UK conditions with RHI subsidy
43 payments included in revenue, but it is debateable whether this is a justifiable technology for public
44 subsidy given its potential for environmental pollution, even after the produced water undergoes
45 treatment. Furthermore, it requires site-dependent investigations that negate the original aim of
46 providing an ‘off the shelf’ geothermal energy source. The hcDGSW variant, with a heat pump used to
47 supplement the heat output of a cDGSW and to lower the reinjection temperature of the circulating
48 fluid as close as possible to the ambient surface temperature (Fig. 2(b)), is shown to have the most
49 potential. The analytical solutions have been used to develop an economic model for this variant,
50 which indicates that the optimal heat output and operating surplus increase with borehole depth to
51 the power of 1.87. This increase is faster than the corresponding increase in drilling costs, indicating

1 that optimal hcDGSW designs will involve boreholes rather deeper than the ~2 km depths considered
 2 hitherto. When RHI subsidy is included, the hcDGSW variant is indeed shown to have the potential for
 3 economic viability, assuming that a heat pump with the specified performance characteristics can be
 4 developed. Moreover, after the timescale for RHI subsidy eligibility has expired, this infrastructure can
 5 be easily repurposed for seasonal heat storage, thus offering the potential of making a significant long-
 6 term contribution to sustainable future heat supply.

8 Acknowledgements

9 The author, who has no conflicts of interest, has been funded in part by European Union Horizon2020
 10 project EC-691728, DESTRESS (DEmonstration of soft Stimulation TREatmentS of geothermal
 11 reservoirS). Any mention of company names or products is for identification purposes only and does
 12 not imply endorsement by the University of Glasgow. Both anonymous reviewers are thanked for their
 13 thoughtful and constructive comments.

15 Glossary

16 Algebraic symbols used in equations in this study are defined here.

| 18 | Symbol | Units | Quantity represented |
|----|---------------|-----------------------------------|--|
| 19 | C | none | Algebraic constant, defined as equal to $\exp(\gamma)$ |
| 20 | D | m | Internal diameter of a pipe |
| 21 | E | J | Heat loss |
| 22 | K | m s^{-1} | Hydraulic conductivity |
| 23 | L | m | Length of a pipe |
| 24 | P_E | £ kWh^{-1} | Unit cost of electrical energy used |
| 25 | P_H | £ kWh^{-1} | Unit cost of heat energy sold |
| 26 | Q | W | Rate of production of heat energy from a DGSW borehole |
| 27 | Q_A | W | Estimate of Q using analytic calculation |
| 28 | Q_G | W | Rate of upward heat flow from below into cylindrical rock volume of radius r_c |
| 29 | Q_N | W | Estimate of Q using numerical modelling |
| 30 | Q_U | W | Rate of production of heat energy that is useable by the associated heat load |
| 31 | Re | none | Reynolds number quantifying the vigour of fluid flow |
| 32 | S | £ | Operating surplus |
| 33 | T | °C | Temperature |
| 34 | T_D | °C | Temperature at which fluid is injected into a DGSW borehole |
| 35 | T_E | °C | Output temperature from a surface heat exchanger or heat pump |
| 36 | T_I | °C | Temperature at which circulating fluid enters a heat pump |
| 37 | T_K | $\text{m}^2 \text{s}^{-1}$ | Hydraulic transmissivity |
| 38 | T_κ | D m | Hydraulic transmissivity |
| 39 | $\%T_K$ | none | Percentage of the total transmissivity of a borehole interval |
| 40 | $\%T_\kappa$ | none | Percentage of the total transmissivity of a borehole interval |
| 41 | T_L | °C | Subsurface temperature at depth z_L |
| 42 | T_o | °C | Temperature at which fluid is produced from a DGSW borehole |
| 43 | T_S | °C | Temperature at the Earth's surface |
| 44 | V | m s^{-1} | Velocity of flow along a pipe |
| 45 | a | m | Radius of a borehole (internal radius of borehole casing) |
| 46 | c | $\text{J kg}^{-1} \text{°C}^{-1}$ | Specific heat capacity |
| 47 | f | none | Ratio, z_L/z_M |
| 48 | f_D | none | Darcy-Weisbach friction factor |
| 49 | f_k | none | Scale factor to incorporate overheads onto the capital cost of a borehole |
| 50 | g | m s^{-2} | Acceleration due to gravity |
| 51 | k | $\text{W m}^{-1} \text{°C}^{-1}$ | Thermal conductivity |

| | | | |
|----|---------------|---------------------|---|
| 1 | q_B | $m^3 s^{-1}$ | Volume flow rate for 'bleed flow' into a DGSW borehole |
| 2 | q_C | $m^3 s^{-1}$ | Volume flow rate for closed-loop circulation in a DGSW borehole |
| 3 | r | m | Radial distance from the axis of a borehole |
| 4 | r_A | m | Radius of influence of fluid production from a well on a surrounding aquifer |
| 5 | r_C | m | Radius of influence of the thermal effect surrounding a DGSW borehole |
| 6 | t | s | Time |
| 7 | t_E | s | Timescale for attainment of steady state conditions around a DGSW |
| 8 | t_L | s | Estimated lifespan of a DGSW project |
| 9 | u | $^{\circ}C km^{-1}$ | Geothermal gradient |
| 10 | w | m | Vertical position below the base of a borehole |
| 11 | x | none | Dimensionless proxy for time |
| 12 | y | none | Dimensionless proxy for temperature variation |
| 13 | z | m | Depth below the Earth's surface |
| 14 | z_L | m | Shallow depth limit for heat production from a DGSW borehole |
| 15 | z_M | m | Depth of the base of a borehole |
| 16 | z_1 | m | Depth of shallow limit of borehole interval |
| 17 | z_2 | m | Depth of deep limit of borehole interval |
| 18 | Γ | none | Ratio, q_B/q_C |
| 19 | ΔH | m | Drawdown to the phreatic surface of an aquifer |
| 20 | ΔH_0 | m | Maximum value of ΔH , at $r=a$ |
| 21 | ΔP | Pa | Pressure drop due to friction at the rim of a pipe |
| 22 | ΔT | $^{\circ}C$ | Temperature change between radius r_C and radius r_A , outside a borehole |
| 23 | Δz | m | Depth interval, z_2-z_1 |
| 24 | Λ | $W m^{-2}$ | Rate of heat production per unit surface area of a borehole |
| 25 | Σ | £ | Capital cost of a borehole |
| 26 | Ψ | none | Coefficient of performance |
| 27 | Ψ_M | none | Mean value of Ψ for a heat pump over a specified temperature range |
| 28 | Ω | none | roughness of the inner surface of a pipe |
| 29 | β | none | Ratio, P_E/P_H |
| 30 | γ | none | Euler's constant |
| 31 | ε | m | Characteristic height of irregularities on the inner surface of a pipe |
| 32 | ζ | $W m^{-1}$ | Rate of heat production per unit depth of a DGSW borehole |
| 33 | ζ_M | $W m^{-1}$ | Value of ζ at depth $z=z_M$ |
| 34 | η | Pa s | The (dynamic) viscosity of a fluid |
| 35 | θ | $^{\circ}$ | Azimuth around a borehole |
| 36 | κ | $mm^2 s^{-1}$ | Thermal diffusivity |
| 37 | κ_P | m^2 | Hydraulic permeability |
| 38 | ρ | $kg m^{-3}$ | Density |
| 39 | χ | none | Dimensionless variable used to specify algebraic functions |

40

41 **References**

- 42 Abesser, C., Lewis, M.A., Marchant, A.P., Hulbert, A.G., 2014. Mapping suitability for open-loop ground
43 source heat pump systems: a screening tool for England and Wales, UK. *Quarterly Journal of*
44 *Engineering Geology and Hydrogeology*, 47, 373–380.
- 45 Abramowitz, M., Stegun, I., 1964. *Handbook of Mathematical Functions with Formulas, Graphs, and*
46 *Mathematical Tables*. Dover, New York.
- 47 AECOM, 2013. *Study into the potential for deep geothermal energy in Scotland: volume 1*. AECOM UK,
48 London, for the Scottish Government, Edinburgh, 216 pp. Available online:
49 <http://www.gov.scot/Resource/0043/00437977.pdf> (accessed 8 March 2018)
- 50 Alimonti, C., Soldo, E., 2016. Study of geothermal power generation from a very deep oil well with a
51 wellbore heat exchanger. *Renewable Energy*, 86, 292-301.

- 1 Alimonti, C., Berardi, D., Bocchetti, D., Soldo, E., 2016. Coupling of energy conversion systems and
2 wellbore heat exchanger in a depleted oil well. *Geothermal Energy*, 4 (11), 17 pp.,
3 doi: 10.1186/s40517-016-0053-9
- 4 Allen, D.J., Brewerton, L.J., Coleby, L.M., Gibbs, B.R., Lewis, M.A., MacDonald, A.M., Wagstaff, S.J.,
5 Williams, A.T., 1997. The physical properties of major aquifers in England and Wales. BGS Technical
6 Report WD/97/34 and Environment Agency R&D Publication 8. British Geological Survey,
7 Keyworth, Nottingham, 333 pp. Available online: <http://nora.nerc.ac.uk/13137/1/WD97034.pdf>
8 (accessed 13 February 2017)
- 9 Atkins, 2013. Deep Geothermal Review Study: Final Report. Atkins Ltd., Epsom, Surrey, for UK
10 Government Department of Energy & Climate Change, 156 pp. Available online:
11 [https://www.gov.uk/government/publications/Deep_Geothermal_Review_Study_Final_Report_F](https://www.gov.uk/government/publications/Deep_Geothermal_Review_Study_Final_Report_Final.pdf)
12 [inal.pdf](https://www.gov.uk/government/publications/Deep_Geothermal_Review_Study_Final_Report_Final.pdf) (accessed 20 February 2017)
- 13 Bailey, M.T., Gandy, C.J., Jarvis, A.P., 2016. Reducing life-cycle costs of passive mine water treatment
14 by recovery of metals from treatment wastes. In: Drebenstedt, C., Paul, M. (eds.), *Mining Meets*
15 *Water – Conflicts and Solutions*. Proceedings of the International Mine Water Association
16 Symposium 2016, Freiberg, Germany, pp. 1255-1262. Available online:
17 https://www.imwa.info/docs/imwa_2016/IMWA2016_Bailey_48.pdf (accessed 17 February 2017)
- 18 Banks, D., 2012. *An Introduction to Thermogeology: Ground Source Heating and Cooling*, 2nd edition.
19 Wiley, Chichester, 544 pp.
- 20 Barelli, A., Palama, A., 1981. A new method for evaluating formation equilibrium temperature in holes
21 during drilling. *Geothermics*, 10, 95-102.
- 22 Barker, J.A., 1986. Modelling of low enthalpy geothermal sources. In: Downing, R.A., Gray, D.A., eds,
23 *Geothermal Energy: the potential in the United Kingdom*. Her Majesty's Stationery Office, London,
24 124-131.
- 25 Barker, J.A., Downing, R.A., Gray, D.A., Findlay, J., Kellaway, G.A., Parker, R.H., Rollin, K.E., 2000.
26 *Hydrogeothermal studies in the United Kingdom*. Quarterly Journal of Engineering Geology and
27 Hydrogeology, 33, 41-58.
- 28 Baster, M.E., 2011. Modelling the performance of air source heat pump systems. M.Sc. thesis,
29 Strathclyde University, Glasgow, Scotland, 82 pp. Available online:
30 http://www.esru.strath.ac.uk/Documents/MSc_2011/Baster.pdf (accessed 14 February 2017)
- 31 Bayer, P., Rivera, J.A., Schweizer, D., Schärli, U., Blum, P., Rybach, L., 2016. Extracting past atmospheric
32 warming and urban heating effects from borehole temperature profiles. *Geothermics*, 64, 289–
33 299.
- 34 Beamish, D., 1990. A deep geoelectric survey of the Carnmenellis granite. *Geophysical Journal*
35 *International*, 102, 679-693.
- 36 Baujard, C., Genter, A., Dalmais, E., Maurer, V., Hehn, R., Rosillette, R., Vidal, J., Schmittbuhl, J., 2017.
37 Hydrothermal characterization of wells GRT-1 and GRT-2 in Rittershoffen, France: Implications on
38 the understanding of natural flow systems in the Rhine Graben, *Geothermics*, 65, 255-268.
- 39 BEIS, 2017. 2015 UK Greenhouse Gas Emissions, Final Figures. UK Government Department of
40 Business, Energy & Industrial Strategy, 54 pp. Available online:
41 [https://www.gov.uk/government/uploads/system/uploads/attachment_data/file/589825/2015](https://www.gov.uk/government/uploads/system/uploads/attachment_data/file/589825/2015_Final_Emissions_statistics.pdf)
42 [Final_Emissions_statistics.pdf](https://www.gov.uk/government/uploads/system/uploads/attachment_data/file/589825/2015_Final_Emissions_statistics.pdf) (accessed 20 February 2017)
- 43 Bloomquist, R.G., 1999. Geothermal heat pumps four plus decades of experience. *GHC Bulletin*,
44 December 1999, 13-27.
- 45 Bourne, S.J., Willemsse, E.J.M., 2001. Elastic stress control on the pattern of tensile fracturing around
46 a small fault network at Nash Point, UK. *Journal of Structural Geology*, 23, 1753-1770.
- 47 Brace, W.F., Walsh, J.B., Frangos, W.T., 1968. Permeability of granite under high pressure. *Journal of*
48 *Geophysical Research*, 73, 2225–2236.
- 49 Bracken, L.J., Bulkeley, H.A., Maynard, C., 2014. Micro-hydro power in the UK: the role of communities
50 in an emerging energy resource. *Energy Policy*, 68, 92-101.

- 1 Bu Xianbiao, Ma Weibin, Li Huashan, 2012. Geothermal energy production utilizing abandoned oil and
2 gas wells. *Renewable Energy*, 41, 80-85.
- 3 Burley, A.J., Edmunds, W.M., Gale, I.N., 1984. Catalogue of Geothermal Data for the Land Area of the
4 United Kingdom. Technical Report WJ/GE/84/020. British Geological Survey, Keyworth,
5 Nottingham, 161 pp. Available online: <http://nora.nerc.ac.uk/id/eprint/512272/1/WJGE84020.pdf>
6 (accessed 7 March 2018)
- 7 Busby, J., Kingdon, A., Williams, J., 2011. The measured shallow temperature field in Britain. *Quarterly*
8 *Journal of Engineering Geology and Hydrogeology*, 44, 373-387.
- 9 Carslaw, H.S., Jaeger, J.C., 1959. *Conduction of heat in solids*. Clarendon Press, Oxford, 510 pp.
- 10 Chadwick, R.A., Holliday, D.W., Holloway, S., Hulbert, A.G., 1995. The structure and evolution of the
11 Northumberland-Solway Basin and adjacent areas. British Geological Survey Subsurface Memoir.
12 HMSO, London, 90 pp.
- 13 Chekhonin, E., Parshin, A., Pissarenko, D., Romushkevich, R., Safonov, S., Spasennykh, M., Chertenkov,
14 M.V., Stenin, V.P., 2012. When rocks get hot: thermal properties of reservoir rocks. *Oilfield Review*,
15 24 (3), 20-37.
- 16 Cheng Wen-Long, Li Tong-Tong, Nian Yong-Le, Wang Chang-Long, 2013. Studies on geothermal power
17 generation using abandoned oil wells. *Energy*, 59, 248-254.
- 18 Cho Jeong-Heum, Nam Yujin, Kim Hyoung-Chan, 2016. Performance and feasibility study of a Standing
19 Column Well (SCW) system using a deep geothermal well. *Energies*, 9, 108, 13 pp.;
20 doi: 10.3390/en9020108
- 21 Collier, R.E.L., 1991. The Lower Carboniferous Stainmore Basin, N. England: extensional basin tectonics
22 and sedimentation. *Journal of the Geological Society*, London, 148, 379-390.
- 23 Collins, G., 2016. Don't ask what wastewater costs but what it's worth.
24 [http://oilprice.com/Energy/Energy-General/Dont-Ask-What-Wastewater-Costs-But-What-its-](http://oilprice.com/Energy/Energy-General/Dont-Ask-What-Wastewater-Costs-But-What-its-Worth.html)
25 [Worth.html](http://oilprice.com/Energy/Energy-General/Dont-Ask-What-Wastewater-Costs-But-What-its-Worth.html) (accessed 14 February 2017)
- 26 Collins, M.A., Law, R., 2017. The development and deployment of deep geothermal single well (DGSW)
27 technology in the United Kingdom. *European Geologist Journal*, 43, 63-68.
- 28 Cornwall, 2017. Historic building pre-application advice for drilling of a geothermal borehole for the
29 use of heating Jubilee Pool, Penzance, Cornwall. Cornwall Council Planning reference
30 PA17/01106/PREAPP. Available online: <http://planning.cornwall.gov.uk/online-applications/>
31 (accessed 14 November 2017)
- 32 Coulton, R., Bullen, C., Dolan, J., Hallett, C., Wright, J., Marsden, C., 2003. Wheal Jane mine water
33 active treatment—design, construction and operation. *Land Contamination & Reclamation*, 11,
34 245–252.
- 35 Dahm, K., Chapman, M., 2014. Produced water treatment primer: case studies of treatment
36 applications. U.S. Department of the Interior, Bureau of Reclamation, Denver, Colorado, 70 pp.
37 Available online: https://www.usbr.gov/research/projects/download_product.cfm?id=1214
38 (accessed 14 February 2017).
- 39 DEA, 2017. Regulation and planning of district heating in Denmark. Danish Energy Agency,
40 Copenhagen, 28 pp. Available online:
41 [https://ens.dk/sites/ens.dk/files/Globalcooperation/regulation_and_planning_of_district_heatin](https://ens.dk/sites/ens.dk/files/Globalcooperation/regulation_and_planning_of_district_heating_in_denmark.pdf)
42 [g_in_denmark.pdf](https://ens.dk/sites/ens.dk/files/Globalcooperation/regulation_and_planning_of_district_heating_in_denmark.pdf) (accessed 28 November 2017).
- 43 DECC, 2012. *The Future of Heating: A strategic framework for low carbon heat in the UK*. Department
44 of Energy and Climate Change, London, 120 pp. Available online:
45 [https://www.gov.uk/government/uploads/system/uploads/attachment_data/file/48574/4805-](https://www.gov.uk/government/uploads/system/uploads/attachment_data/file/48574/4805-future-heating-strategic-framework.pdf)
46 [future-heating-strategic-framework.pdf](https://www.gov.uk/government/uploads/system/uploads/attachment_data/file/48574/4805-future-heating-strategic-framework.pdf) (accessed 26 February 2017)
- 47 DECC, 2016a. Quarterly Energy Prices, 30 June 2016. UK Government Department of Energy & Climate
48 Change, 39 pp. Available online:
49 [https://www.gov.uk/government/uploads/system/uploads/attachment_data/file/532712/QEP_J](https://www.gov.uk/government/uploads/system/uploads/attachment_data/file/532712/QEP_June_2016_Final.pdf)
50 [une_2016_Final.pdf](https://www.gov.uk/government/uploads/system/uploads/attachment_data/file/532712/QEP_June_2016_Final.pdf) (accessed 20 February 2017)

- 1 DECC, 2016b. UK Energy Statistics, 2015 & Q4 2015. UK Government Department of Energy & Climate
2 Change, 16 pp. Available online:
3 [https://www.gov.uk/government/uploads/system/uploads/attachment_data/file/513244/Press](https://www.gov.uk/government/uploads/system/uploads/attachment_data/file/513244/Press_Note_March_2016.pdf)
4 [Notice_March_2016.pdf](https://www.gov.uk/government/uploads/system/uploads/attachment_data/file/513244/Press_Note_March_2016.pdf) (accessed 20 February 2017)
- 5 DEFRA, 2011. Environmental permitting guidance, radioactive substances regulation; for the
6 Environmental Permitting (England and Wales) Regulations 2010. UK Government Department for
7 Environment, Food and Rural Affairs, London, 89 pp. Available online:
8 [https://www.gov.uk/government/uploads/system/uploads/attachment_data/file/69503/pb1363](https://www.gov.uk/government/uploads/system/uploads/attachment_data/file/69503/pb1363_2-ep-guidance-rsr-110909.pdf)
9 [2-ep-guidance-rsr-110909.pdf](https://www.gov.uk/government/uploads/system/uploads/attachment_data/file/69503/pb1363_2-ep-guidance-rsr-110909.pdf) (accessed 25 February 2017)
- 10 DEFRA, 2014. Water Framework Directive implementation in England and Wales: new and updated
11 standards to protect the water environment. UK Government Department for Environment, Food
12 and Rural Affairs, London, 41 pp. Available online:
13 [https://www.gov.uk/government/uploads/system/uploads/attachment_data/file/307788/river-](https://www.gov.uk/government/uploads/system/uploads/attachment_data/file/307788/river-basin-planning-standards.pdf)
14 [basin-planning-standards.pdf](https://www.gov.uk/government/uploads/system/uploads/attachment_data/file/307788/river-basin-planning-standards.pdf) (accessed 25 February 2017)
- 15 Deng Zheng, Rees, S.J., Spitler, J.D., 2005. A model for annual simulation of standing column well
16 ground heat exchangers. *International Journal of Heating, Ventilating, Air-Conditioning and*
17 *Refrigerating Research*, 11 (4), 637-655.
- 18 Donselaar, M.E., Groenenberg, R.M., Gilding, D.T., 2015. Reservoir geology and geothermal potential
19 of the Delft Sandstone Member in the West Netherlands Basin. *Proceedings, World Geothermal*
20 *Congress 2015, Melbourne, Australia, 19-25 April 2015*, paper 12054, 9 pp.
- 21 Downing, R.A., 1986. Engineering and economic aspects of low enthalpy development. In: Downing,
22 R.A., Gray, D.A., eds, *Geothermal Energy: the potential in the United Kingdom*. Her Majesty's
23 Stationery Office, London, pp. 148-151.
- 24 Downing, R.A., Allen, D.J., Barker, J.A., Burgess, W.G., Gray, D.A., Price, M., Smith, I.F., 1984.
25 Geothermal exploration at Southampton in the UK: a case study of a low enthalpy resource. *Energy*
26 *Exploration & Exploitation*, 2, 327-342.
- 27 DTI, 1999. *New and Renewable Energy: Prospects for the 21st Century*. Department of Trade and
28 Industry, London, 70 pp. Available online:
29 [http://webarchive.nationalarchives.gov.uk/20000817030113/http://www.dti.gov.uk:80/renew/c](http://webarchive.nationalarchives.gov.uk/20000817030113/http://www.dti.gov.uk:80/renew/condoc/)
30 [ondoc/](http://webarchive.nationalarchives.gov.uk/20000817030113/http://www.dti.gov.uk:80/renew/condoc/) (accessed 23 November 2017)
- 31 East Ayrshire, 2017. Screening Request for proposed deep geothermal single well; Kilmarnock, East
32 Ayrshire. East Ayrshire Council pre-screening planning application 17/0009/EIASCR. Available
33 online: [https://www.east-ayrshire.gov.uk/PlanningAndTheEnvironment/Planning-](https://www.east-ayrshire.gov.uk/PlanningAndTheEnvironment/Planning-applications/Planning-applications.aspx)
34 [applications/Planning-applications.aspx](https://www.east-ayrshire.gov.uk/PlanningAndTheEnvironment/Planning-applications/Planning-applications.aspx) (accessed 14 November 2017)
- 35 Edmunds, W.M., 1975. Geochemistry of brines in the coal measures of Northeast England.
36 *Transactions of the Institution of Mining and Metallurgy, London (Section B: Applied Earth Science)*,
37 84, B39-B52.
- 38 Edmunds, W.M., 1986. Geochemistry of geothermal waters in the UK. In: Downing, R.A., Gray, D.A.,
39 eds, *Geothermal Energy: the potential in the United Kingdom*. Her Majesty's Stationery Office,
40 London, pp. 111-123.
- 41 EIA, 2016. Carbon Dioxide Emissions Coefficients. U.S. Energy Information Administration,
42 Washington, DC. Available online:
43 https://www.eia.gov/environment/emissions/co2_vol_mass.cfm (accessed 10 March 2017)
- 44 Enggcyclopedia, 2011. Absolute Pipe Roughness. Available online:
45 <http://www.enggcyclopedia.com/2011/09/absolute-roughness/> (accessed 14 November 2017)
- 46 England, P.C., Oxburgh, E.R., Richardson, S.W., 1980. Heat refraction and heat production in and
47 around granite plutons in north-east England. *Geophysical Journal International*, 62, 439-455.
- 48 Förster, H.-J., 1999. The chemical composition of uraninite in Variscan granites of the Erzgebirge,
49 Germany. *Mineralogical Magazine*, 63, 239-252.
- 50 Förster, H.-J., Tischendorf, G., Trumbull, R.B., Gottesmann, B., 1999. Late-collisional granites in the
51 Variscan Erzgebirge, Germany. *Journal of Petrology*, 40, 1613-1645.

- 1 GEL, 2014. 2 October 2014: First deep geothermal energy produced in Cornwall for 25 years.
2 Geothermal Engineering Ltd., London. Available online:
3 <http://www.geothermalengineering.co.uk/news.php> (accessed 20 February 2017)
- 4 GEL, University of St Andrews, & Arup, 2016. Feasibility report of a deep geothermal single well,
5 Aberdeen Exhibition and Conference Centre. Scottish Government, Edinburgh, 103 pp. Available
6 online: <http://www.gov.scot/Resource/0049/00497878.pdf> (accessed 20 February 2017)
- 7 Geon, 2017. September 2017: Scotland's first deep geothermal district heating network. Geon Energy
8 Ltd., London. Available online: http://geonenergy.com/wordpress/geonenergy_news/ (accessed
9 17 November 2017)
- 10 Gillespie, M.R., Crane, E.J., Barron, H.F., 2013. Study into the potential for deep geothermal energy in
11 Scotland: volume 2. Scottish Government, Edinburgh, 125 pp. Available online:
12 <http://www.gov.scot/Resource/0043/00437996.pdf> (accessed 13 February 2018)
- 13 Groves, P., Hochwimmer, A., Seastres Jr., J., 2012. A pre-feasibility study for energy recovery from
14 geothermal prospects in Scotland. In: Proceedings, New Zealand Geothermal Workshop 2012.
15 Auckland, New Zealand, 19-21 November 2012, 7 pp.
- 16 Hamm, S.-Y., Kim, M.S., Cheong, J.-Y., Kim, J.-Y., Son, M., Kim, T.-W., 2007. Relationship between
17 hydraulic conductivity and fracture properties estimated from packer tests and borehole data in
18 a fractured granite. *Engineering Geology*, 92, 73-87.
- 19 Hepbasli, A., 2005. Thermodynamic analysis of a ground-source heat pump system for district heating.
20 *International Journal of Energy Research*, 29, 671-687.
- 21 Illman, W.A., Liu, X., Takeuchi, S., Yeh, T.-C.J., Ando, K., Saegusa, H., 2009. Hydraulic tomography in
22 fractured granite: Mizunami underground research site, Japan. *Water Resources Research*, 45,
23 W01406, 18 pp., doi: 10.1029/2007WR006715.
- 24 Johnson, D.B., Hallberg, K.B., 2005. Acid mine drainage remediation options: a review. *Science of the*
25 *Total Environment*, 338, 3-14.
- 26 Johnson, G.A.L., Somerville, I.D., Tucker, M.E., Cózar, P., 2011. Carboniferous stratigraphy and context
27 of the Seal Sands No. 1 Borehole, Teesmouth, NE England: the deepest onshore borehole in Great
28 Britain. *Proceedings of the Yorkshire Geological Society*, 58, 173-196.
- 29 Johnston, D., Potter, H., Jones, C., Rolley, S., Watson, I., Pritchard, J., 2008. Abandoned mines and the
30 water environment. Science project SC030136-41. The Environment Agency, Bristol, 40 pp.
31 Available online:
32 https://www.gov.uk/government/uploads/system/uploads/attachment_data/file/8879_df7d5c.pdf (accessed 25
33 February 2017)
- 34 Joule, 2017. Underfloor heating. Joule UK Ltd., Bromborough, England, 24 pp. Available online:
35 <http://www.jouleuk.co.uk/wp-content/uploads/2015/09/Joule-Underfloor-Heating-Brochure.pdf>
36 (accessed 28 November 2017)
- 37 Kavanaugh, S., Green, M., Mescher, K., 2012. Long-term commercial GSHP performance. Part 4:
38 Installation costs. *ASHRAE Journal*, 54 (10), 26-36. Available online: [www.geokiss.com/tech-
39 notes/LongTermGSHPsPt4.pdf](http://www.geokiss.com/tech-notes/LongTermGSHPsPt4.pdf) (accessed 16 July 2017)
- 40 Kiessig, G., Gatzweiler, R., Jakubick, A.T., 2004. Remediation options and the importance of water
41 treatment at former uranium production sites in eastern Germany. In: *Treatment of Liquid Effluent*
42 *from Uranium Mines and Mills*, IAEA-TECHDOC-1419. International Atomic Energy Agency, Vienna,
43 pp. 127-143. Available online: www-pub.iaea.org/MTCD/publications/PDF/te_1419_web.pdf
44 (accessed 16 February 2017).
- 45 King, D., Browne, J., Layard, R., O'Donnell, G., Rees, M., Stern, N. & Turner, A. 2015. A Global Apollo
46 Programme to Combat Climate Change. Centre for Economic Performance, London School of
47 Economics and Political Science, 40 pp. Available online:
48 http://cep.lse.ac.uk/pubs/download/special/Global_Apollo_Programme_Report.pdf (accessed 2
49 March 2017)

- 1 Knight Piesold and partners, 1995. Wheal Jane Minewater Study: Environmental Appraisal and
2 Treatment Strategy. Knight Piesold Ltd, Ashford, Kent, 446 pp. Available online:
3 <http://www.environmentdata.org/fedora/repository/ealit:2627/OBJ/20000033.pdf> (accessed 17
4 February 2017)
- 5 Knight Piesold and partners, 1998. Wheal Jane Minewater Project: Consultancy Studies 1996-1999.
6 Appraisal and Selection of Long Term Treatment Option. Knight Piesold Ltd, Ashford, Kent, 183 pp.
7 Available online: <http://ea-lit.freshwaterlife.org/archive/ealit:1620/OBJ/20000888.pdf> (accessed
8 17 February 2017)
- 9 KÜchler, A., Kiessig, G., Kunze, C., 2005. Passive biological treatment systems of mine waters at
10 WISMUT sites. Proceedings, 9th International Congress on Mine Water & the Environment, Oviedo,
11 Spain, pp. 361-368. Available online:
12 https://www.imwa.info/docs/imwa_2005/IMWA2005_051_Kuechler.pdf (accessed 16 February
13 2017).
- 14 Kunze, C., KÜchler, A., 2003. Passive biological treatment systems of mine waters at WISMUT sites.
15 Proceedings, 8th International Congress on Mine Water & the Environment, Johannesburg, South
16 Africa, pp. 187-199. Available online: [https://www.imwa.info/docs/imwa_2003/imwa_2003_187-
17 199.pdf](https://www.imwa.info/docs/imwa_2003/imwa_2003_187-199.pdf) (accessed 16 February 2017).
- 18 Law, R., 2014. Deep Geothermal Heat Production – Single Well Trial. In: Renewable Heating &
19 Renewable Cooling; Ground Source Heat Pump Association 5th Technical Seminar, De Montfort
20 University, Leicester, 16 November 2014, 8 pp. Available online:
21 <http://www.gshp.org.uk/DeMontfort/GeothermalEngineeringLtd.pdf> (accessed 20 February 2017)
- 22 Law, R., Bridgland, D., Nicholson, D., Chendorain, M., 2015. Heat extraction from deep single wells.
23 Proceedings World Geothermal Congress 2015. Melbourne, Australia, 19-25 April 2015.
24 <https://pangea.stanford.edu/ERE/db/WGC/papers/WGC/2015/28002.pdf>
- 25 Lee, M.K., 1986. Hot dry rock. In: Downing, R.A., Gray, D.A., eds, Geothermal Energy: the potential in
26 the United Kingdom. Her Majesty's Stationery Office, London, pp. 21-41.
- 27 Lee, M.K., Brown, G.C., Webb, P.C., Wheildon, J., Rollin, K.E., 1987. Heat flow, heat production and
28 thermo-tectonic setting in mainland UK. Journal of the Geological Society, London, 144, 35-42.
- 29 Lewis, M.A., Cheney, C.S., O'Dochartaigh, B.E., 2006. Guide to permeability indices. BGS Open Report
30 CR/06/160N, British Geological Survey, Keyworth, Nottingham, 29 pp. Available online:
31 <http://nora.nerc.ac.uk/7457/1/CR06160N.pdf> (accessed 13 February 2017)
- 32 Liu Xiaobing, Hughes, P., Anderson, A., 2016. An overview of geothermal heat pump applications and
33 a preliminary assessment of its technical potential in the United States. GRC Transactions, 40, 707-
34 716.
- 35 Lockett, G.E., 1986. Single borehole geothermal energy extraction system for electrical power
36 generation. Proceedings, Eleventh Workshop on Geothermal Reservoir Engineering, Stanford
37 University, Stanford, California, 21-23 January 1986. SGP-TR-93, 2 pp. Available online:
38 <https://www.geothermal-energy.org/pdf/IGAstandard/SGW/1986/Lockett.pdf> (accessed 25
39 February 2017)
- 40 Lyons, W.C., Go BoYun, Graham, R.L., Hawley, G.D., 2009. Air and Gas Drilling Manual: Applications for
41 Oil and Gas Recovery Wells and Geothermal Fluids Recovery Wells. Elsevier, Amsterdam.
- 42 McCay, A.T., 2016. Heat production measurements from Scottish granites. Available online:
43 <http://researchdata.gla.ac.uk/id/eprint/302> (accessed 2 March 2017)
- 44 McDermott, C.I., Randriamanjatoa, A.L., Tenzer, H., Kolditz, O., 2006. Simulation of heat extraction
45 from crystalline rocks: the influence of coupled processes on differential reservoir cooling.
46 Geothermics, 35, 321-344.
- 47 McGarr, A., Gay, N.C., 1978. State of stress in the Earth's crust. Annual Review of Earth and Planetary
48 Sciences, 6, 405-436.
- 49 McKeon, B.J., Swanson, C.J., Zagarola, M.V., Donnelly, R.J., Smits, A.J., 2004. Friction factors for smooth
50 pipe flow. Journal of Fluid Mechanics, 511, 41-44.

- 1 Manetti, G., 1973. Attainment of temperature equilibrium in holes during drilling. *Geothermics*, 2, 94-
2 100.
- 3 Manning, D.A.C., Younger, P.L., Smith, F.W., Jones, J.M., Dufton, D.J., Diskin, S., 2007. A deep
4 geothermal exploration well at Eastgate, Weardale, UK: a novel exploration concept for low-
5 enthalpy resources. *Journal of the Geological Society, London*, 164, 371–382.
- 6 Martinez-Landa, L., Carrera, J., 2005. An analysis of hydraulic conductivity scale effects in granite (Full-
7 scale Engineered Barrier Experiment (FEBEX), Grimsel, Switzerland). *Water Resources Research*,
8 41, W03006, 13 pp., doi: 10.1029/2004WR003458 (with 2005 correction: *Water Resources*
9 *Research*, 41, W11703, 1 p., doi: 10.1029/2005WR004446).
- 10 Met Office, 2017. Aberdeen Airport climate. UK Meteorological Office, Exeter. Available online:
11 <http://www.metoffice.gov.uk/public/weather/climate/gfnmmyh91> (accessed 2 March 2017).
- 12 Moody, L.F., 1944. Friction factors for pipe flow. *Transactions of the American Society of Mechanical*
13 *Engineers*, 66, 671–684.
- 14 Morris, J., 2014. Pumping the polluted water from mines. BBC News. Available online:
15 <http://www.bbc.co.uk/news/uk-england-26573994> (accessed 17 February 2017).
- 16 Nalla, G., Shook, G.M., Mines, G.L., Bloomfield, K., 2004. Parametric sensitivity study of operating and
17 design variables in wellbore heat exchangers. *Proceedings, Twenty-Ninth Workshop on*
18 *Geothermal Reservoir Engineering Stanford University, Stanford, California, 26-28 January 2004*,
19 SGP-TR-175, 9 pp. Available online:
20 <http://citeseerx.ist.psu.edu/viewdoc/download?doi=10.1.1.545.9839&rep=rep1&type=pdf>
21 (accessed 16 July 2017).
- 22 Noorollahi, Y., Bina, S.M., Yousefi, H., 2016. Simulation of power production from dry geothermal well
23 using down-hole heat exchanger in Sabalan Field, northwest Iran. *Natural Resources Research*, 25,
24 227-239.
- 25 OFGEM, 2017. Feed-In Tariff (FIT) rates. Office of Gas and Electricity Markets, London. Available online:
26 <https://www.ofgem.gov.uk/environmental-programmes/fit/fit-tariff-rates> (accessed 21
27 November 2017).
- 28 O’Neill, Z.D., Spitler, J.D., Rees, S.J., 2006. Modeling of standing column wells in ground source heat
29 pump systems. *ASHRAE Transactions*, 101 (1), 173-185. Available online:
30 [http://www.hvac.okstate.edu/sites/default/files/pubs/papers/2006/05-
31 Oneill_Spitler_Rees_06.pdf](http://www.hvac.okstate.edu/sites/default/files/pubs/papers/2006/05-Oneill_Spitler_Rees_06.pdf) (accessed 16 July 2017).
- 32 ONS, 2017. Population estimates for UK, England and Wales, Scotland and Northern Ireland, mid-2016.
33 UK Office for National Statistics, London. Available online:
34 [https://www.ons.gov.uk/peoplepopulationandcommunity/populationandmigration/populationes
35 timates/datasets/populationestimatesforukenglandandwalesscotlandandnorthernireland](https://www.ons.gov.uk/peoplepopulationandcommunity/populationandmigration/populationestimates/datasets/populationestimatesforukenglandandwalesscotlandandnorthernireland)
36 (accessed 28 November 2017).
- 37 Orio, C.D., Johnson, C.N., Rees, S.J., Chiasson, A., Deng Zheng, Spitler, J.D., 2005. A survey of standing
38 column well installations in North America. *ASHRAE Transactions*, 111 (2), 109-121. Available
39 online: [http://www.hvac.okstate.edu/sites/default/files/pubs/papers/2005/05-
40 Orio_Johnson_Rees_Chiasson_Deng_Spitler_05.pdf](http://www.hvac.okstate.edu/sites/default/files/pubs/papers/2005/05-Orio_Johnson_Rees_Chiasson_Deng_Spitler_05.pdf) (accessed 16 July 2017).
- 41 Peacock, C., 2014. Pumping water from disused UK mines. Available online:
42 <http://www.aquaread.com/pumping-water-disused-uk-mines/> (accessed 17 February 2017).
- 43 Rafferty, K. 2001. Design aspects of commercial open-loop heat pump systems. *Geo-Heat Center*
44 *Quarterly Bulletin*, 22, 16–24.
- 45 Ramaekers, J., Geel, K., Lokhorst, A., Simmelink, H.J., 2006. Nader onderzoek naar mogelijkheden van
46 aardwarmtewinning voor de vleestomaatwekerij van Fa A&G van den Bosch BV te Bleiswijk.
47 Report 2006-U-R0016/B, 71 pp. Nederlandse Organisatie voor Toegepast Natuurwetenschappelijk
48 Onderzoek, Utrecht, the Netherlands. Available online:
49 [http://nlog.nl/cmis/browser?id=workspace%3A//SpacesStore/5355c256-c291-4204-bb52-
50 fda100f91327](http://nlog.nl/cmis/browser?id=workspace%3A//SpacesStore/5355c256-c291-4204-bb52-fda100f91327) (accessed 28 January 2017)

- 1 Renewables First, 2015. How much hydropower income would my system provide? Renewables First
2 Ltd., Stroud, Gloucestershire. Available online:
3 [http://www.renewablesfirst.co.uk/hydropower/hydropower-learning-centre/how-much-income-](http://www.renewablesfirst.co.uk/hydropower/hydropower-learning-centre/how-much-income-would-my-hydro-system-provide/)
4 [would-my-hydro-system-provide/](http://www.renewablesfirst.co.uk/hydropower/hydropower-learning-centre/how-much-income-would-my-hydro-system-provide/) (accessed 21 November 2017)
- 5 Rees, S.J., Spitler, J.D., Deng Zheng, Orio, C.D., Johnson, C.N., 2004. A study of geothermal heat pump
6 and standing column well performance. ASHRAE Transactions 110 (1), 3-13. Available online:
7 [http://www.hvac.okstate.edu/sites/default/files/pubs/papers/2004/06-](http://www.hvac.okstate.edu/sites/default/files/pubs/papers/2004/06-Rees_Spitler_Deng_Orio_Johnson_04.pdf)
8 [Rees Spitler Deng Orio Johnson 04.pdf](http://www.hvac.okstate.edu/sites/default/files/pubs/papers/2004/06-Rees_Spitler_Deng_Orio_Johnson_04.pdf) (accessed 16 July 2017).
- 9 Riahi, A., Moncarz, P., Kolbe, W., Damjanac, B., 2017. Innovative closed-loop geothermal well designs
10 using water and super critical carbon dioxide as working fluids. Proceedings, Forty-second
11 Workshop on Geothermal Reservoir Engineering, Stanford University, Stanford, California, 13-15
12 February 2017. SGP-TR-212, 9 pp. Available online:
13 <https://pangea.stanford.edu/ERE/db/GeoConf/papers/SGW/2017/Riahi.pdf> (accessed 16 July
14 2017).
- 15 Richards, H.G., Parker, R.H., Green, A.S.P., Jones, R.H., Nicholls, J.D.M., Nicol, D.A.C., Randall, T.M.M.,
16 Richards, S., Stewart, R.C., Willis-Richards, J., 1994. The performance and characteristics of the
17 experimental Hot Dry Rock geothermal reservoir at Rosemanowes, Cornwall (1985-1988).
18 Geothermics, 23, 73-109.
- 19 Rollin, K.E., 1995. A simple heat-flow quality function and appraisal of heat-flow measurements and
20 heat-flow estimates from the UK Geothermal Catalogue. Tectonophysics, 244, 185-196.
- 21 Rybach, L., Eugster, W.J., Hopkirk, R.J., Kaelin, B., 1992. Borehole heat exchangers: longterm
22 operational characteristics of a decentral geothermal heating system. Geothermics, 21, 861-867.
- 23 Satman, A., 2011. Sustainability of geothermal doublets. Proceedings, Thirty-Sixth Workshop on
24 Geothermal Reservoir Engineering, Stanford University, Stanford, California, 31 January - 2
25 February 2011. SGP-TR-191, 9 pp. Available online:
26 <https://pangea.stanford.edu/ERE/pdf/IGAstandard/SGW/2011/satman.pdf> (accessed 14 July
27 2017)
- 28 Simmelink, H.J., Geel, K., 2008. Sustainable tomatoes are growing on geothermal heat. Nederlandse
29 Organisatie voor Toegepast Natuurwetenschappelijk Onderzoek, Utrecht, the Netherlands.
30 Available online: <https://www.tno.nl/media/2629/information20-art1.pdf> (accessed 28 January
31 2017)
- 32 Smit, R.C.A., 2012. Optimisation of geothermal well doublet placement. M.Sc. thesis, Technical
33 University Delft, Delft, the Netherlands. Available online:
34 <https://repository.tudelft.nl/islandora/object/uuid%3A09d6081e-33ab-4511-8c5e-31016f841716>
35 (accessed 14 July 2017)
- 36 Smith, I.F., 1986. Mesozoic basins. In: Downing, R.A., Gray, D.A., eds, Geothermal Energy: the potential
37 in the United Kingdom. Her Majesty's Stationery Office, London, pp. 42-83.
- 38 Snow, D.T., 1969. Anisotropic permeability of fractured media. Water Resources Research, 5, 1273-
39 1289.
- 40 Spitler, J.D., Javed, S., Kalskin Ramstad, R., 2016. Natural convection in groundwater-filled boreholes
41 used as ground heat exchangers. Applied Energy, 164, 352-365.
- 42 Tenzer, H., Park Chan-Hee, Kolditz, O., McDermott, C.I., 2010, Application of the geomechanical facies
43 approach and comparison of exploration and evaluation methods used at Soultz-sous-Forêts
44 (France) and Spa Urach (Germany) geothermal sites. Environmental Earth Sciences, 61, 853-880.
- 45 Thiem, G., 1906. Hydrologische Methoden. J.M. Gebhardt, Leipzig, Germany, 56 pp.
- 46 van Wees, J.D.A.M., Kramers, L., Kronimus, R.A., Pluymaekers, M.P.D., Mijnlieff, H.F., Vis, G.J., 2010.
47 ThermoGIS™ V1.0: Part II: Methodology. Nederlandse Organisatie voor Toegepast
48 Natuurwetenschappelijk Onderzoek (TNO; Netherlands Organisation for Applied Scientific
49 Research), Utrecht, the Netherlands, 61 pp. Available online:
50 www.thermogis.nl/downloads/ThermoGISmanual_partII.pdf (accessed 21 February 2017)

- 1 Vidal, J., Genter, A., Schmittbuhl, J., 2016. Pre- and post-stimulations of the geothermal well GRT-1
2 (Rittershoffen, France): insights from acoustic image logs on hard fractured rock investigations,
3 Geophysical Journal International, 206, 845-860.
- 4 Voss, C.I., Provost, A.M., 2010. SUTRA: A model for saturated-unsaturated, variable-density ground-
5 water flow with solute or energy transport. Water-Resources Investigations Report 02-4231. U.S.
6 Geological Survey, Reston, Virginia, 300 pp.
- 7 Wang Zhe, 2009. Modeling study of a single-well enhanced geothermal system (EGS). Proceedings,
8 Thirty-fourth Workshop on Geothermal Reservoir Engineering Stanford University, Stanford,
9 California, 9-11 February 2009. SGP-TR-190, 81 pp. Available online:
10 <https://pangea.stanford.edu/ERE/research/geoth/publications/.../SGP-TR-190.pdf> (accessed 16
11 July 2017)
- 12 Wang Zhe, McClure, M.W., Horne, R.N., 2010. Modeling study of single-well EGS configurations.
13 Proceedings World Geothermal Congress 2010, Bali, Indonesia, 25-29 April 2010, paper 3113, 12
14 pp. Available online: <https://www.geothermal-energy.org/pdf/IGAstandard/WGC/2010/3113.pdf>
15 (accessed 16 July 2017)
- 16 Westaway, R., 2016. Repurposing of disused shale gas wells for subsurface heat storage: preliminary
17 analysis concerning UK issues. Quarterly Journal of Engineering Geology and Hydrogeology, 49,
18 213–227.
- 19 Westaway, R., Younger, P.L., 2013. Accounting for palaeoclimate and topography: a rigorous approach
20 to correction of the British geothermal dataset. Geothermics, 48, 31-51.
- 21 Westaway, R., Younger, P.L., 2016. Unravelling the relative contributions of climate change and
22 ground disturbance to subsurface temperature perturbations: case studies from Tyneside, UK.
23 Geothermics, 64, 490–515.
- 24 Wheildon, J., Rollin, K.E., 1986. Engineering and economic aspects of low enthalpy development. In:
25 Downing, R.A., Gray, D.A., eds, Geothermal Energy: the potential in the United Kingdom. Her
26 Majesty's Stationery Office, London, pp. 8-20.
- 27 Younger, P.L., 2000. The adoption and adaptation of passive treatment technologies for mine waters
28 in the United Kingdom. Mine Water and the Environment, 19, 85-97.
- 29 Younger, P.L., 2014. Hydrogeological challenges in a low-carbon economy. Quarterly Journal of
30 Engineering Geology and Hydrogeology, 47, 7-27.
- 31 Younger, P.L., Banwart, S.A., Hedin, R.S., 2002. Mine Water: Hydrology, Pollution, Remediation.
32 Kluwer, Dordrecht, the Netherlands, 464 pp.
- 33 Younger, P.L., Coulton, R.H., Froggatt, E.C., 2005. The contribution of science to risk-based decision-
34 making: Lessons from the development of full-scale treatment measures for acidic mine waters at
35 Wheal Jane, UK. Science of the Total Environment, 338, 137-154.
- 36 Younger, P.L., Manning, D.A.C., 2010. Hyper-permeable granite: lessons from test-pumping in the
37 Eastgate Geothermal Borehole, Weardale, UK. Quarterly Journal of Engineering Geology and
38 Hydrogeology, 43, 5–10.
- 39 Younger, P.L., Manning, D.A.C., Millward, D., Busby, J.P., Jones, C.R.C., Gluyas, J.G., 2016. Geothermal
40 exploration in the Fell Sandstone Formation (Mississippian) beneath the city centre of Newcastle
41 upon Tyne, UK: the Newcastle Science Central Deep Geothermal Borehole. Quarterly Journal of
42 Engineering Geology and Hydrogeology, 49, 350-363.

43

44

45 **Table 1 – on a separate sheet.**

Table 2: Estimates of cDGSW performance

| | Q (kW) | T _o (5 yrs) (°C) | Q _u (5 yrs) (kW) | T _o (10 yrs) (°C) | Q _u (10 yrs) (kW) | T _o (20 yrs) (°C) | Q _u (20 yrs) (kW) |
|---|-----------|--------------------------------|--------------------------------|---------------------------------|---------------------------------|---------------------------------|---------------------------------|
| <i>z_M=2000 m; T_L=30 °C; T_M=74 °C (f≈0.31)</i> | | | | | | | |
| 0 | | 74.0 | 0.0 | 74.0 | 0.0 | 74.0 | 0.0 |
| 20 | | 66.9 | 13.0 | 66.5 | 12.9 | 66.0 | 12.9 |
| 40 | | 59.9 | 24.0 | 59.0 | 23.7 | 58.0 | 23.3 |
| 60 | | 52.8 | 32.0 | 51.5 | 31.1 | 50.0 | 30.0 |
| 80 | | 45.8 | 35.3 | 44.0 | 32.9 | 42.0 | 30.0 |
| 100 | | 38.3 | 29.3 | 36.6 | 24.8 | 34.0 | 16.7 |
| 120 | | 31.7 | 9.4 | 29.1 | 0.0 | 26.0 | 0.0 |
| <i>z_M=2500 m; T_L=30 °C; T_M=90 °C (f=0.25)</i> | | | | | | | |
| 0 | | 90.0 | 0.0 | 90.0 | 0.0 | 90.0 | 0.0 |
| 20 | | 84.8 | 14.7 | 84.5 | 14.6 | 84.1 | 14.6 |
| 40 | | 79.7 | 28.5 | 79.0 | 28.4 | 78.3 | 28.3 |
| 60 | | 74.5 | 41.4 | 73.5 | 41.1 | 72.4 | 40.8 |
| 80 | | 69.3 | 53.0 | 68.0 | 52.4 | 66.6 | 51.7 |
| 100 | | 64.2 | 63.1 | 62.6 | 62.0 | 60.7 | 60.6 |
| 120 | | 59.0 | 71.0 | 57.0 | 68.9 | 54.9 | 66.5 |
| 140 | | 53.8 | 76.1 | 51.5 | 72.5 | 49.0 | 68.2 |
| 160 | | 48.6 | 77.1 | 46.0 | 71.1 | 43.2 | 63.6 |
| 180 | | 43.5 | 72.5 | 40.6 | 62.4 | 37.3 | 48.1 |
| 200 | | 38.3 | 58.7 | 35.1 | 40.6 | 31.4 | 13.1 |
| 220 | | 33.2 | 30.3 | 29.6 | 0.0 | 25.5 | 0.0 |
| <i>z_M=3000 m; T_L=30 °C; T_M=106 °C (f≈0.21)</i> | | | | | | | |
| 0 | | 106.0 | 0.0 | 106.0 | 0.0 | 106.0 | 0.0 |
| 20 | | 101.9 | 15.6 | 101.7 | 15.6 | 101.4 | 15.6 |
| 40 | | 97.9 | 30.9 | 97.3 | 30.8 | 96.8 | 30.8 |
| 60 | | 93.8 | 45.7 | 93.0 | 45.5 | 92.1 | 45.4 |
| 80 | | 89.7 | 59.9 | 88.7 | 59.7 | 87.5 | 59.4 |
| 100 | | 85.6 | 73.5 | 84.3 | 73.1 | 82.9 | 72.6 |
| 120 | | 81.5 | 86.4 | 80.0 | 85.7 | 78.3 | 84.9 |
| 140 | | 77.5 | 98.5 | 75.6 | 97.3 | 73.6 | 96.0 |
| 160 | | 73.4 | 109.5 | 71.3 | 107.8 | 69.0 | 105.8 |
| 180 | | 69.3 | 119.3 | 66.9 | 116.7 | 64.4 | 113.8 |
| 200 | | 65.2 | 127.5 | 62.6 | 124.0 | 59.7 | 119.5 |
| 220 | | 61.1 | 133.9 | 58.3 | 128.9 | 55.1 | 122.4 |
| 240 | | 57.0 | 137.9 | 53.9 | 130.7 | 50.5 | 121.5 |
| 260 | | 52.9 | 138.8 | 49.6 | 128.7 | 45.9 | 115.2 |
| 280 | | 48.9 | 136.0 | 45.3 | 121.4 | 41.3 | 101.1 |
| 300 | | 44.8 | 127.6 | 41.0 | 106.5 | 36.6 | 74.4 |
| 320 | | 40.7 | 111.5 | 36.6 | 79.4 | 32.0 | 29.1 |
| 340 | | 36.6 | 84.4 | 32.3 | 35.1 | 27.4 | 0.0 |
| 360 | | 32.6 | 41.4 | 28.0 | 0.0 | 22.8 | 0.0 |

Calculations, on the basis explained in the main text, demonstrating the performance issues that result for cDGSW installations operated at nonzero values of f . Values of useable heat output Q_u and output temperature T_o after 5, 10 and 20 years of operation are listed. The calculations assume $a=0.1$ m, $T_s=10$ °C, $u=32$ °C km⁻¹, $k=3.5$ W m⁻¹ °C⁻¹, and $\kappa=1.2$ mm² s⁻¹ (cf. Fig. 4).

1 **Table 3:** Hydraulic transport properties of granites: on a separate sheet.

2
3 **Table 4:** Temperatures at 1 km depth: on a separate sheet.

6 **Figure Captions**

7 **Figure 1.** Schematic diagrams depicting groundwater extraction DGSWs. Thin solid arrows indicate
8 directions of fluid flow; the fluid is shaded to convey an impression of its temperature and/or whether
9 it is warming or cooling at each point in the model. Temperatures at key points are labelled for
10 comparison with the main text. (a) A simple wDGSW in which hot water is pumped out of a permeable
11 aquifer, is cooled by transferring heat to working fluid (which supplies heat to a heat load), then the
12 resulting warm water is discharged into the environment. (b) A hwDGSW, in which after passing
13 through the heat exchanger the ground water is cooled further using a heat pump. The Southampton
14 geothermal project, discussed in the text, operated as in (a) from 1988 to 1991 then was modified as
15 in (b). It does not incorporate treatment of the discharged water but this is depicted schematically as
16 it will arguably be necessary for any future projects of this type.

17
18 **Figure 2.** Schematic diagrams depicting conductive DGSWs, using the same notation as in Fig. 1 plus
19 broad open arrows indicate directions of heat conduction in the subsurface. (a) A cDGSW, in which
20 the borehole contains part of a closed circulation loop. Note that with this variant much of the heat
21 produced (at temperature T_0) is not used, because the output temperature of the heat exchanger, T_E ,
22 and thus the reinjection temperature T_D of the circulating fluid, significantly exceeds the ambient
23 surface temperature T_S . This heat is reinjected and warms the subsurface down to depth z_L where the
24 initial rock temperature T_L equals the fluid temperature $T_E (=T_D)$. The circulating fluid is thus warmed
25 between depth z_L and the well bottom at z_M , not throughout the full vertical extent of the borehole
26 (the parameter f , which appears in equations defined in the text, being the ratio z_L/z_M). To the best of
27 my knowledge, this system design was first proposed by Rybach et al. (1992). (b) A hcDGSW, in which
28 a heat pump is added to the closed-loop configuration in (a), to supplement the useful heat output by
29 cooling the circulating fluid to the ambient temperature T_S . This also increases the proportion of the
30 borehole available for heat production. This configuration, not previously analysed in detail, is
31 favoured in the present study as the preferred DGSW variant.

32
33 **Figure 3.** Schematic diagrams depicting 'dual mode' DGSWs, combining the option of water extraction
34 (with the deeper part of the borehole open to its surroundings) with heat production by conduction,
35 using the same notation as in Fig. 2. (a) A dDGSW, in which ground water is drawn into the borehole
36 heat exchanger at depth and discharged at the surface, potentially increasing the thermal output. This
37 variant suffers from the principal disadvantages in Fig. 2(a), that reinjection of warm water reduces
38 the output of useful heat and warms the surroundings of the shallow part of the borehole, limiting the
39 proportion of it available for heat production. It also introduces other disadvantages, including the
40 need for relatively permeable bedrock at depth, scaling of the pipe loop due to precipitation of
41 substances dissolved in the circulating ground water, the need for treatment of the discharged water,
42 and associated regulatory issues. (b) A hdDGSW, in which a heat pump is added to the configuration
43 in (a), to supplement the useful heat output by cooling the circulating fluid to the ambient
44 temperature T_S . This also increases the proportion of the borehole available for heat production.
45 However, the difficulties remain over identification of permeable bedrock and disposal of the ground
46 water that is discharged into the environment. A system of this type is proposed at the AECC (GEL et
47 al., 2016).

1 **Figure 4.** Calculated variations in output temperature T_o for a cDGSW operating for 10 years at
2 constant rates of heat production Q 50, 80, 140 and 260 kW, assuming $z_M=2500$ m, $T_M=80$ °C, $T_S=0$ °C,
3 $a=0.1$ m, $k=3.5$ W m⁻¹ °C⁻¹, $\kappa=1.2$ mm² s⁻¹, and $f=0$, based on equations (4) and (5) (open symbols). For
4 comparison, solid and dashed lines indicate variations in T_o for a cDGSW with $z_M=2500$ m, $T_M=80$ °C,
5 and $T_S=0$ °C, operating for 10 years with heat production at $Q=50, 100, 200$ and 400 kW, according to
6 Fig. 5 of Law et al. (2015). See text for discussion.
7

8 **Figure 5.** Predicted temperature variations at depth $z_M=2500$ m as a function of radial distance r ,
9 calculated using equations (4) and (5) for $Q=50$ kW at different times after the start of cDGSW
10 operation. The other model parameters are as described for Fig. 4; linear ((a)) and logarithmic ((b))
11 scales for radial distance are used. Note that, for reasons discussed in the text, the calculated values
12 of $r=r_c$ at which the cooling effect reaches zero (respectively, 2.2, 4.6, 9.2, 18.5, 29.2 and 41.3 m) are
13 approximate and underestimate the actual radial distance at which this effect becomes infinitesimally
14 small by a factor of \sqrt{C} or ~ 1.33 . Note, also, that despite the low rate of heat production assumed, the
15 borehole does not reach a thermal steady state on any of the timescales depicted (cf. Law et al., 2015).
16

17 **Figure 6.** Graphs of the notional project lifespan t_L (calculated using equation (9)) for cDGSWs with
18 $a=0.1$ m in a region with $T_S=10$ °C, $u=32$ °C km⁻¹, $k=3.5$ W m⁻¹ °C⁻¹, and $\kappa=1.2$ mm² s⁻¹. **(a)** For
19 $z_M=2000$ m, so $T_M=74$ °C; the values of $f=0.0, 0.2, 0.4$ and 0.6 correspond to $T_L=10.0, 22.8, 35.6,$ and
20 48.4 °C. For $f=0.6$, $t_L=20$ years corresponds to $Q=43$ kW. **(b)** For $z_M=2500$ m, so $T_M=90$ °C; the values of
21 $f=0.0, 0.15, 0.3$ and 0.45 correspond to $T_L=10.0, 22.0, 34.0,$ and 46.0 °C. For $f=0.45$, $t_L=20$ years
22 corresponds to $Q=125$ kW. **(c)** For $z_M=3000$ m, so $T_M=106$ °C; the values of $f=0.0, 0.1, 0.2$ and 0.3
23 correspond to $T_L=10.0, 19.6, 29.2,$ and 48.4 °C. For $f=0.3$, $t_L=20$ years corresponds to $Q=286$ kW.
24

25 **Figure 7.** Depictions of the potential cost-effectiveness of hcDGSW boreholes for 20 years of operation
26 with different values of z_M as a function of rates of heat supply to the associated heat load. **(a)** 2000
27 m; **(b)** 2500 m; **(c)** 3000 m; **(d)** 4000 m. Calculations assume $T_S=10$ °C, $u=32$ °C km⁻¹, $a=0.1$ m,
28 $k=3.5$ W m⁻¹ °C⁻¹, $\kappa=1.2$ mm² s⁻¹, $T_E=T_D=40$ °C, $L=z_M$ (i.e., boreholes are vertical), $\rho=1000$ kg m⁻³,
29 $c=4186$ J kg⁻¹ °C⁻¹, $D=0.04$ m, and $\Omega=5 \times 10^{-5}$, with heat and electricity pricing, subsidy payments, and
30 other input parameters as described in the text. Dashed horizontal lines denote estimated capital
31 costs; dashed vertical lines denote optimum solutions, at 193 kW in (a), 295 kW in (b), 416 kW in (c),
32 and 711 kW in (d). Note that at power outputs of ≥ 213 kW in (a), ≥ 326 kW in (b), ≥ 465 kW in (c), and
33 808 kW in (d), greater financial returns would result from ending operation before 20 years have
34 elapsed, because in the later stages of operation T_o is predicted to fall so low (<15.7 °C in (a), <18.2 °C
35 in (b), <20.9 °C in (c), and <27.1 °C in (d)) that Ψ declines sufficiently for the cost of the electricity used
36 to exceed the value of the heat produced, even with RHI subsidy included.
37

38 **Figure 8.** Comparison between calculations of heat production from a cDGSW calculated using
39 equations (4) and (5) with the outputs in Fig. 5 of Law et al. (2015) (cf. Fig. 4). Both sets of outputs
40 have been converted to dimensionless variables x and y (defined in the text), where x is a proxy for
41 time and y is a proxy for the fall over time in the output temperature. The calculations of $\Delta T(z_M)$, using
42 equations (4) and (5), and the transformation to dimensionless variables utilise the following
43 parameter values: $z_M=2500$ m, $T_M=80$ °C, and $T_S=0$ °C (all specified by Law et al., 2015), along with
44 $a=0.1$ m, $k=3.5$ W m⁻¹ °C⁻¹, $\kappa=1.2$ mm² s⁻¹, and $f=0$. See text for discussion.
45

46 **Figure 9.** Variations over time in T_o for the optimum hcDGSW configurations from Fig. 7. After T_o falls
47 below T_E it is assumed that all the heat output is via the heat pump, with the heat exchanger bypassed
48 (cf. Fig. 2(b)). Crosses mark the times when the three setups become uneconomic in the absence of
49 RHI subsidy (i.e., when the operating cost first exceeds the revenue from sale of heat). These are: for
50 $T_o \leq 21.8$ °C (after ~ 17 years) for $z_M=2000$ m; $T_o \leq 25.7$ °C (after ~ 18.5 years) for $z_M=2500$; $T_o \leq 29.9$ °C
51 (after 20 years) for $z_M=3000$ m; and $T_o \leq 38.8$ °C (after ~ 25 years) for $z_M=4000$ m.
52
53

1 **Figure 10.** Comparison of rates of heat output, for 10 years of operation, of cDGSW installations,
2 predicted by the present analytic model (Q_A) and by numerical models. The present analytic models
3 are adjusted to give the same values of T_O as the extant numerical models. Data points (Q_A , Q_N , in kW)
4 are (50, 50), (80, 100), (140, 200), and (260, 400), based on comparison with Law et al. (2015), and
5 (530, 1200), based on comparison with Alimonti et al. (2016). Values for all model parameters are
6 noted in the text. The trend line defined in equation (34) is also depicted.

7
8 **Figure 11.** Summary estimates for the technical and economic performance of the HALO hcDGSW
9 project in Kilmarnock, Scotland. **(a)** Graphs of predicted temperature decline, calculated using the
10 same procedure as for Fig. 4. The calculations assume different values of Q , with $T_M=69$ °C, $T_S=T_D=9$ °C,
11 $T_E=70$ °C, $f=0$, $a=0.375$ m, $u=26$ °C km⁻¹, $k=4$ W m⁻¹ °C⁻¹, and $\kappa=1.5$ mm² s⁻¹. **(b)** Graphs of predicted
12 economic performance, calculated using the same operational parameters as for part (a) and the same
13 economic model as for Fig. 7. See text for discussion.

14
15 **Figure 12.** Revision to Fig. 11 for $a=0.1$ m instead of 0.375 m.

16
17 **Figure 13.** Summary estimates for the technical and economic performance of a hypothetical hcDGSW
18 project in Darlington, northeast England. **(a)** Graphs of predicted temperature decline, calculated
19 using the same procedure as for Fig. 4. The calculations assume different values of Q , with $z_M=6000$ m,
20 $T_M=279$ °C, $T_S=T_D=9$ °C, $T_E=35$ °C, $f=0$, $a=0.1$ m, $u=45$ °C km⁻¹, $k=1.7$ W m⁻¹ °C⁻¹, and $\kappa=0.9$ mm² s⁻¹. **(b)**
21 Graphs of predicted economic performance, calculated using the same operational parameters as for
22 part (a) and the same economic model as for Fig. 7. See text for discussion.

23
24
25

Table 1: Summary of DGSW technology variants

| Notation | Illustration | Description |
|----------|--------------|---|
| wDGSW | Fig. 1(a) | Open-loop design in which hot water is produced, flows through a heat exchanger, and is then discharged into the environment circa the rejection temperature of the heat exchanger. Corresponds to the Southampton project in its original form. Requires permeable bedrock; in the UK requires regulatory approval for the discharge, which will limit future applicability. |
| hwDGSW | Fig. 1(b) | Open-loop design in which hot water is produced and flows through a heat exchanger, before being cooled further to near-ambient temperature using a heat pump, then discharged into the environment. Corresponds to the Southampton project in its present, modified, form. Requires permeable bedrock; in the UK requires regulatory approval for the discharge, which will limit future applicability. In the USA, shallow versions of this design are known as open loop groundwater heat pump systems. |
| cDGSW | Fig. 2(a) | Closed-loop design in which water circulates through a borehole, passing through a heat exchanger at the surface, re-entering the borehole circa the rejection temperature of the heat exchanger. Subsurface heat flow to and from the borehole is by conduction only, so the design imposes no constraints on bedrock permeability. However, the reinjection above ambient temperature means that some of the heat produced contributes to heating the bedrock at shallow depths, limiting the usefulness of this design (and favouring the hcDGSW variant, discussed below, instead). I am not aware of any deep geothermal project that uses this variant, although it has featured in desk studies (e.g., by Law et al., 2015). |
| hcDGSW | Fig. 2(b) | Closed-loop design in which water circulates through a borehole, passing through a heat exchanger then a heat pump at the surface, re-entering the borehole near ambient temperature. The surface heat exchanger is bypassed if the produced water is below its reject temperature. Subsurface heat flow to and from the borehole is by conduction only, so the design imposes no constraints on bedrock permeability. I am not aware of any deep geothermal project that uses this variant, which is investigated in detail in the present study given its future potential. Excluding the surface heat exchanger, this design is equivalent to an upscaled (deep geothermal) version of what is known in the UK a ground source heat pump system and in the USA a closed loop ground coupled heat pump system. |
| dDGSW | Fig. 3(a) | Open-loop design in which water circulates through a borehole, passing through a heat exchanger at the surface, re-entering the borehole circa the rejection temperature of the heat exchanger, supplemented by flow bled from groundwater then discharged into the environment. Requires permeable bedrock; in the UK requires regulatory approval for the discharge, which will limit future applicability. I am not aware of any deep geothermal project that uses this variant, although it has featured in desk studies (e.g., by Law et al., 2015). |
| hdDGSW | Fig. 3(b) | Open-loop design in which water circulates through a borehole, passing through a heat exchanger then a heat pump at the surface, re-entering the borehole near ambient temperature, supplemented by flow bled from groundwater then discharged into the environment. The surface heat exchanger is bypassed if the produced water is below its reject temperature. Requires permeable bedrock; in the UK requires regulatory approval for the discharge, which will limit future applicability. I am not aware of any deep geothermal project that uses this variant, although it has featured in desk studies (e.g., by GEL et al., 2016). Excluding the surface heat exchanger, this design is equivalent to an upscaled (deep geothermal) version of what is known in the USA a standing column well groundwater heat pump system. |

Details summarized here are discussed at length in the text. U.S. terminology is from Deng et al. (2005).

Table 3: Hydraulic transport properties of granites

| Depth (MD) | | Depth (TVD) | | Δz (m) | T (°C) | η (mPa s) | %T _κ | %T _K | T _κ (D m) | T _K (m ² s ⁻¹) | κ _p (m ²) | K (m s ⁻¹) |
|--------------------------|-----------------------|-----------------------|-----------------------|-------------------|-----------|-------------------|-----------------|-----------------|-------------------------|---|-------------------------------------|---------------------------|
| z ₁ (m) | z ₂ (m) | z ₁ (m) | z ₂ (m) | | | | | | | | | |
| <i>Rosemanowes RH-15</i> | | | | | | | | | | | | |
| 2130 | 2374 | 2054 | 2273 | 219 | 55 | 0.507 | 12 | 16.20 | 0.113 | 2.18×10 ⁻⁶ | 5.16×10 ⁻¹⁶ | 9.99×10 ⁻⁹ |
| 2374 | 2395 | 2273 | 2292 | 19 | 65 | 0.436 | 59 | 68.48 | 0.477 | 1.07×10 ⁻⁵ | 2.51×10 ⁻¹⁴ | 5.65×10 ⁻⁷ |
| 2395 | 2415 | 2292 | 2310 | 18 | 68 | 0.417 | 12 | 11.76 | 0.093 | 2.18×10 ⁻⁶ | 5.16×10 ⁻¹⁵ | 1.21×10 ⁻⁷ |
| 2415 | 2466 | 2310 | 2356 | 46 | 78 | 0.365 | 0 | 0.00 | - | - | - | - |
| 2466 | 2490 | 2356 | 2376 | 20 | 80 | 0.355 | 12 | 11.34 | 0.079 | 2.18×10 ⁻⁶ | 3.95×10 ⁻¹⁵ | 1.09×10 ⁻⁷ |
| 2490 | 2700 | 2376 | 2565 | 189 | 95 | 0.299 | 5 | 3.98 | 0.028 | 9.10×10 ⁻⁷ | 1.47×10 ⁻¹⁶ | 4.81×10 ⁻⁹ |
| | | | | 511 | | | 100 | 100 | 0.790 | 1.82×10 ⁻⁵ | | |
| <i>Eastgate-1</i> | | | | | | | | | | | | |
| 410 | 432 | 410 | 432 | 22 | 26 | 0.880 | 99 | 99.34 | 3920 | 4.37×10 ⁻² | 1.78×10 ⁻¹⁰ | 1.99×10 ⁻³ |
| 432 | 995 | 432 | 995 | 563 | 27 | 0.859 | 1 | 0.66 | 25.6 | 2.92×10 ⁻⁴ | 4.55×10 ⁻¹⁴ | 5.19×10 ⁻⁷ |
| | | | | 585 | | | 100 | 100 | 3925 | 4.40×10 ⁻² | | |

Here, z_1 and z_2 denote the depth limits above and below each interval of each borehole, in terms of both Measured Depth (MD) and True Vertical Depth (TVD). The Eastgate-1 borehole is vertical so these measures of depth are equivalent. Δz is the difference between z_2 and z_1 measured as TVD. T is a representative temperature of the water in each interval. η is the viscosity of water at temperature T. T_κ and %T_κ are the transmissivity of each interval and its percentage of the total transmissivity, expressed as $\kappa_p \times \Delta z$, where κ_p is the permeability of the interval. T_K and %T_K are the transmissivity of each interval and its percentage of the total transmissivity, expressed as $K \times \Delta z$, where K is the hydraulic conductivity of the interval. Data (i.e., the stated values for z_1 , z_2 , T, %T_κ, and T_κ) are from Richards et al. (1994) for the Carnmenellis Granite (in the Rosemanowes RH-15 borehole, Cornwall), and from Manning et al. (2007) and Younger and Manning (2010) for the Weardale Granite (in the Eastgate-1 borehole, County Durham). The other parameters are calculated as part of the present study, using standard formulae for the inter-relationships between the quantities listed. See text for discussion.

Table 4. Subsurface temperatures

| Locality | Population | T (°C) | Ref. | Note |
|---|------------|--------|------|------|
| <i>Northern and North-central England</i> | | | | |
| Darlington | 105,600 | 54 | B | |
| Harrogate | 156,300 | 52 | B | |
| Leeds | 781,700 | 50 | B | |
| Wakefield | 336,800 | 50 | B | |
| Bury | 188,700 | 50 | B | |
| Rochdale | 216,200 | 49 | B | |
| Newcastle upon Tyne | 296,500 | 48 | Y | |
| Barnsley | 241,200 | 48 | B | |
| Oldham | 232,700 | 48 | B | |
| Gateshead | 201,600 | 48 | Y | |
| Stockton-on-Tees | 195,700 | 48 | B | |
| Sheffield | 575,400 | 46 | B | |
| Manchester | 541,300 | 46 | B | |
| Bradford | 534,300 | 46 | B | |
| Huddersfield | 437,000 | 46 | B | 1 |
| Hull | 260,200 | 46 | B | |
| Ashton-under-Lyne | 223,200 | 46 | B | 2 |
| Middlesbrough | 140,400 | 46 | B | |
| Lichfield | 103,100 | 46 | B | |
| Stockport | 290,600 | 45 | B | |
| Chesterfield | 104,400 | 44 | B | |
| Nottingham | 325,300 | 42 | B | |
| Bolton | 283,100 | 42 | B | |
| Walsall | 278,700 | 42 | B | |
| Rotherham | 261,900 | 42 | B | |
| Derby | 256,200 | 42 | B | |
| Salford | 248,700 | 42 | B | |
| Trafford | 234,700 | 42 | B | 3 |
| York | 208,400 | 42 | B | |
| Grimsby | 159,100 | 42 | B | 4 |
| Mansfield | 107,400 | 42 | B | |
| <i>Wessex Basin and surroundings</i> | | | | |
| Southampton | 254,300 | 48 | B | |
| Eastleigh | 129,600 | 48 | B | |
| Winchester | 122,000 | 48 | B | |
| Chichester | 118,200 | 48 | B | |
| Tunbridge Wells | 117,100 | 48 | B | |
| Eastbourne | 103,100 | 48 | B | |
| Bournemouth | 197,700 | 46 | B | |
| Maidstone | 166,400 | 46 | B | |
| Poole | 151,500 | 46 | B | |
| Tonbridge | 127,300 | 46 | B | |
| Sevenoaks | 119,100 | 46 | B | |
| Fareham | 115,400 | 46 | B | |
| Crawley | 111,400 | 46 | B | |
| Basingstoke | 174,600 | 44 | B | |
| Havant | 123,600 | 44 | B | |
| Worthing | 108,600 | 44 | B | |

| | | | | |
|------------|---------|----|---|---|
| Croydon | 382,300 | 42 | B | 5 |
| Bromley | 326,900 | 42 | B | 5 |
| Brighton | 289,200 | 42 | B | 6 |
| Greenwich | 279,800 | 42 | B | 5 |
| Medway | 278,500 | 42 | B | |
| Plymouth | 264,200 | 42 | B | |
| Bexley | 244,800 | 42 | B | 5 |
| Portsmouth | 214,800 | 42 | B | |
| Sutton | 202,200 | 42 | B | 5 |
| Thurrock | 167,000 | 42 | B | |
| Horsham | 138,000 | 42 | B | |
| Torbay | 133,900 | 42 | B | |
| Gravesend | 106,800 | 42 | B | 7 |
| Dartford | 105,500 | 42 | B | 5 |
| Lewes | 101,400 | 42 | B | |

Values of the temperature T, measured or estimated at 1 km depth, from Busby et al. (2011) (B) or Younger et al. (2016) (Y), are plotted for towns and cities in Britain with populations >100,000 (population data from ONS, 2017). The values reported were measured by Younger et al. (2016) beneath Newcastle upon Tyne and are assumed beneath neighbouring Gateshead. These relatively high temperatures, listed, arise due to combinations of relatively high heat flow and/or relatively low thermal conductivity sediments, including thick sequences of Carboniferous mudstone in sedimentary basins in northern and central England. Sites are grouped geographically; no localities in Scotland or Wales have high enough subsurface temperatures for inclusion, whereas Northern Ireland has not been assessed. Annual mean surface temperatures are within $\sim\pm 1$ °C of 10 °C at almost all localities listed, so geothermal gradients in the uppermost 1 km beneath the Earth's surface can be readily calculated approximately. Notes: 1, Kirklees Metropolitan Borough (MB); 2, Tameside MB; 3, Trafford MB; 4, North East Lincolnshire Unitary local Authority (UA); 5, London Borough; 6, Brighton & Hove UA; 7, Gravesham District.

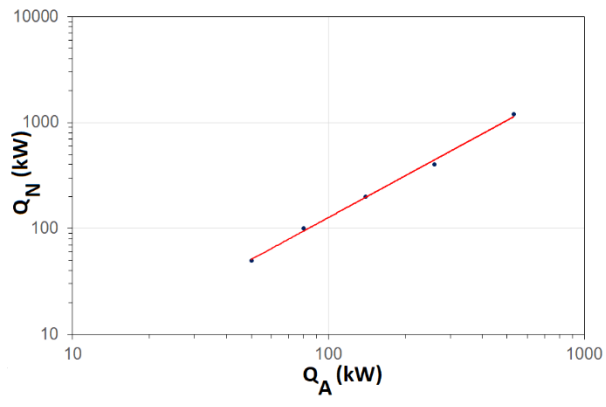
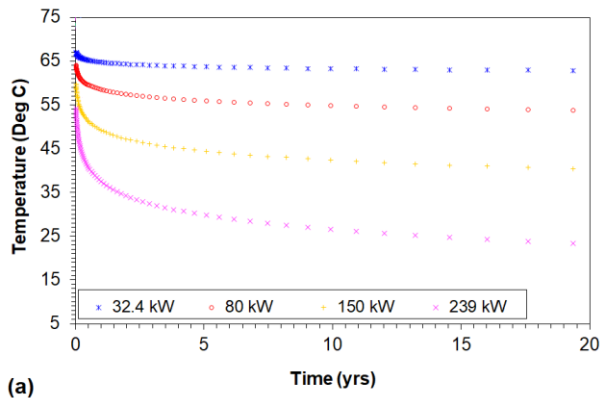
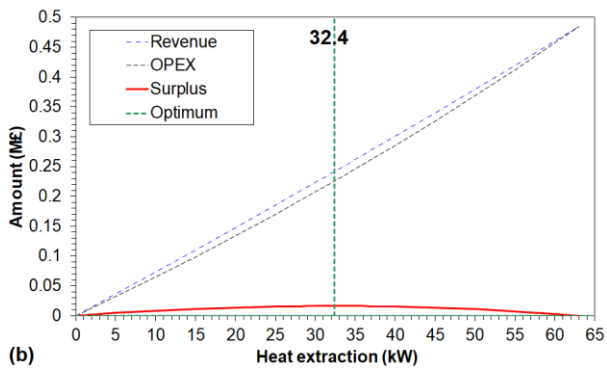


Figure 10

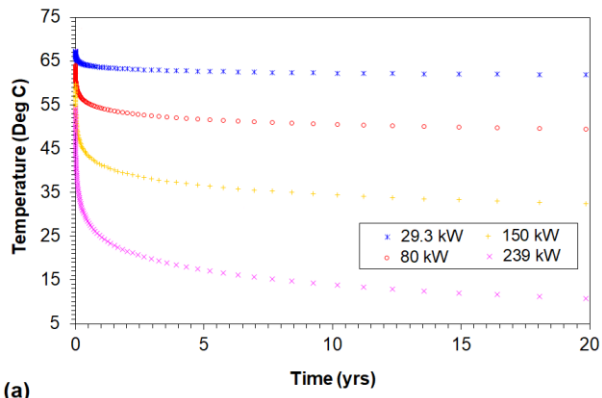


(a)

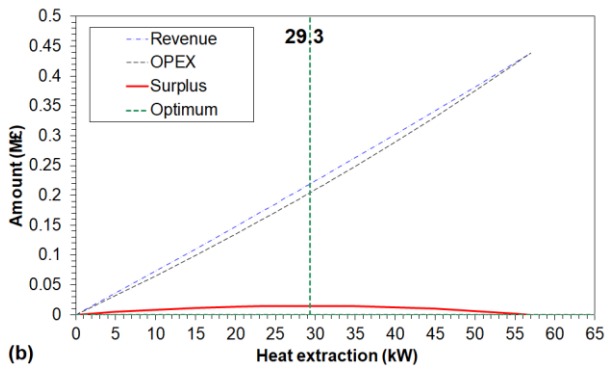


(b)

Figure 11

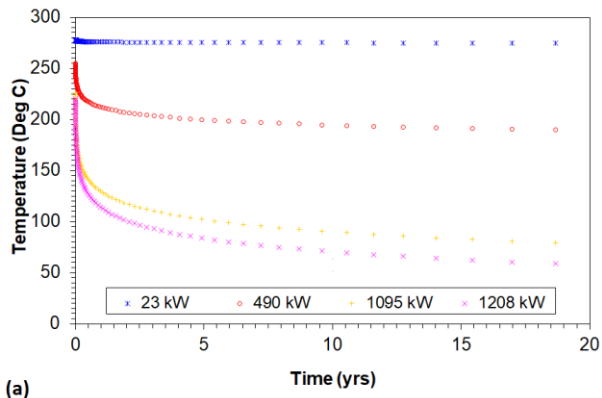


(a)

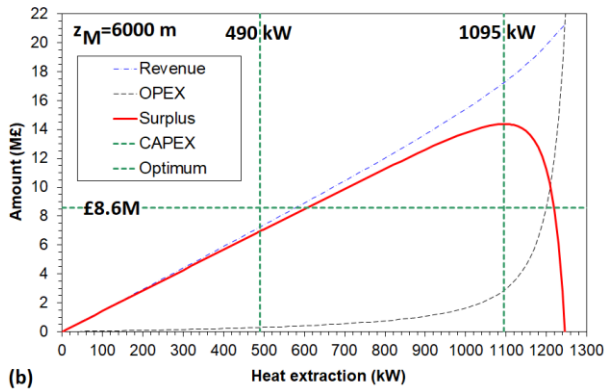


(b)

Figure 12



(a)



(b)

Figure 13